CHEMOSTRATIGRAPHY OF THE UPPER CRETACEOUS FROM CENTRAL AND SOUTH TEXAS WITH FOCUS ON THE EAGLE FORD GROUP

by

BRETT HUFFMAN

Presented to the Faculty of the Graduate School of
The University of Texas at Arlington in Partial Fulfillment
of the Requirements
for the Degree of

MASTER OF SCIENCE IN GEOLOGY

THE UNIVERSITY OF TEXAS AT ARLINGTON
AUGUST 2013

ACKNOWLEDGEMENTS

I would like to thank my wife, children, and parents for their constant support as we have traveled down the path that I have chosen. The patience and constant love of my wife has served as my rock and kept my focus clear. I also give heartfelt thanks to my advisor, Dr. Harry Rowe, for his honest and straightforward guidance, his willingness to offer insight, and for taking this graduate student under his wing, helping me realize my dream of attaining a graduate degree in the field of geology.

I would also like to thank Dr. John Wickham for all of his guidance and wisdom throughout my journey as a graduate student, as well as his involvement as one of my thesis committee members. I would also like to thank Dr. Andrew Hunt for agreeing to be a member of my thesis committee. Dr. Steve Ruppel has been very valuable through correspondence and as a facilitator for my many trips to Austin, helping to ensure that the cores I needed access to were readily available. I would also like to thank the staff at the B.E.G. core repository, Nathan Ivicic especially, for their flexibility, good humor, and for making sure my cores were pulled and ready for my many last-minute trips to collect data.

I would also like to thank Steve Wilson and Laurie Van Ingen for their support in my endeavor to better myself, their advice, and their friendship.

July 22, 2013

ABSTRACT

CHEMOSTRATIGRAPHY OF THE UPPER CRETACEOUS
FROM CENTRAL AND SOUTH TEXAS WITH
FOCUS ON THE EAGLE FORD GROUP

Brett Huffman, M.S.

The University of Texas at Arlington, 2013

Supervising Professor: Harold Rowe

The fine-grained organic-rich rocks of the Eagle Ford (Cenomanian-Turonian) were deposited during the Upper Cretaceous in the shallow waters of the Western Interior Seaway. Five drill cores recovered from two counties, four from Travis County, Texas and one from Frio County, Texas, have been scanned from between two foot and half foot intervals with a hand-held energy-dispersive x-ray fluorescence (HH-ED-XRF) spectrometer to acquire major (e.g. Ca, Si, Al) and trace (e.g. Mo, V, Ni) element data for quantitative analysis. Additionally, gamma ray logs have been analyzed for two of the cores.

Major element geochemistry indicates the Eagle Ford deposited in South Texas is different from the Eagle Ford deposited in Central Texas. South Texas Eagle Ford is much more Ca (carbonate) rich, with a noticeably lower Al (clay) content. South Texas and Central Texas Eagle Ford both have low Si (quartz) content relative to the Al and Ca content, indicating a negligible siliciclastic contribution during deposition. Trace element analysis reveals the redox conditions of the bottom waters during deposition. Mn -- an element which becomes mobile and may be removed from an open system in reducing conditions -- levels are much higher in the

Austin Chalk and Buda with notably lower values in the Eagle Ford in both Central Texas and South Texas. Mo, an element which tends to bind with organic matter or sulfides during reducing conditions, is notably higher in the Eagle Ford of both South Texas and Central Texas. The correlation of decreased Mn levels and increased Mo levels suggests that the Eagle Ford was deposited in reducing conditions in an open system capable of removing mobilized Mn.

Geochemical analysis of major and trace elements obtained from ED-XRF may be used in the petroleum industry in concert with XRD, electric logs, and standard core analysis to give a more complete picture of the depositional environment, clay type and volume, geophysical rock properties, and areal extent of a potential unconventional shale reservoir for hydrocarbon extraction. XRF data offers insight about the rocks, leading to improved understanding of the depositional environment and chemical makeup. Applying these technologies to the Eagle Ford helps unlock the potential of this significant hydrocarbon source and reservoir.

TABLE OF CONTENTS

LIST OF ILLUSTRATIONS

LIST OF TABLES

CHAPTER 1

INTRODUCTION

1.1 Purpose of Study

Fossil fuels are a very significant source of the worlds' energy. As the population of the planet increases, so do the demands for energy. Although alternative energy sources are being developed, it is understood that they are not ready to step in and replace fossil fuels. Current estimates of global fossil fuel consumption are in excess of seven billion barrels of oil equivalent, and are projected to increase to 31 – 47 billion barrels of oil equivalent per year by 2040 (Assareh, Behrang, Assareh, Hedayat, 2011). In order to meet these growing demands, the petroleum industry has begun the search for more energy from unconventional sources. A large part of the development of unconventional resources is an increased cost of development. Hydraulic fracturing has become an indispensable completion technique for unconventional hydrocarbon recoveries, but the cost is very high.

Mudrocks are of increasing economic importance, with impetus from increasing unconventional hydrocarbon production from black shales (Tourtelot, 1979). Since Josef Pompeckj first posited that organic rich shales deposited in euxinic waters could potentially be source rock for hydrocarbons (Brumsack, 2006), the idea that shales are of economic importance has grown. Energy prices and increased demand has helped stimulate the development of technology and has led to a recent progression in the study of these important resources. As a better understanding of shales is fostered, this knowledge may be applied toward more efficient exploitation and development of these resources, helping to contribute to the growing global energy demands.

1.2 Study Area and Regional Geology

The Cretaceous period is recognized as a time of increased tectonic activity and associated volcanism which resulted in higher levels of CO_2, leading to increased global temperatures and a lack of polar ice and continental glaciers (Barron, 1983). The rock record from the Cretaceous indicates the presence of a shallow seaway cutting NNE-SSW across present day North America (**Figure 1**). The Western Interior Seaway was the likely the result of the confluence of warmer climate and increased tectonism which led to higher-than-normal rock volume production at the mid-Atlantic spreading center, and were filled with warm, organic rich waters (Mancini and Pucket, 2005). Once the extra CO_2 generated from the increased volcanic activity was converted back into organic material, the system returned to "normal" operational mode (Brumsack, 2006).

Warmer waters resulted in the loss of the oceanic circulation responsible for the normal cycling of oxygen rich waters and nutrient rich waters which typically lead to modern oceanic conditions. Stratification of the Cretaceous waters was caused by the lack of regular cycling of shallow and deep waters. Stratified water columns may lead to anoxic water bottom conditions, identified in the rock record by the presence of anoxia proxies. In the mid-Cretaceous, several distinct periods of organic-rich black shale deposition appear (Hetzel, Böttcher, Wortmann, and Brumsack, 2009). These periods of increased organic-rich shale deposition are referred to as Oceanic Anoxic Events (OAE, Schlanger and Jenkyns, 1976). The OAE that took place at the C/T boundary, known as OAE 2, is a focal point of study in the geochemical analysis of the cores scanned from Travis and Frio counties, Texas, with minor emphasis placed on the overlying and underlying formations. The Austin Chalk unconformably overlies the Eagle Ford shale and is composed of very high percentages of carbonates with some minor percentages of shale, represented as thin beds. The Eagle Ford is largely represented by the presence of organic-rich shale and varying concentrations of carbonate. The Buda is unconformably overlain by the Eagle Ford, and consists almost entirely of carbonate (**Figure 2**).

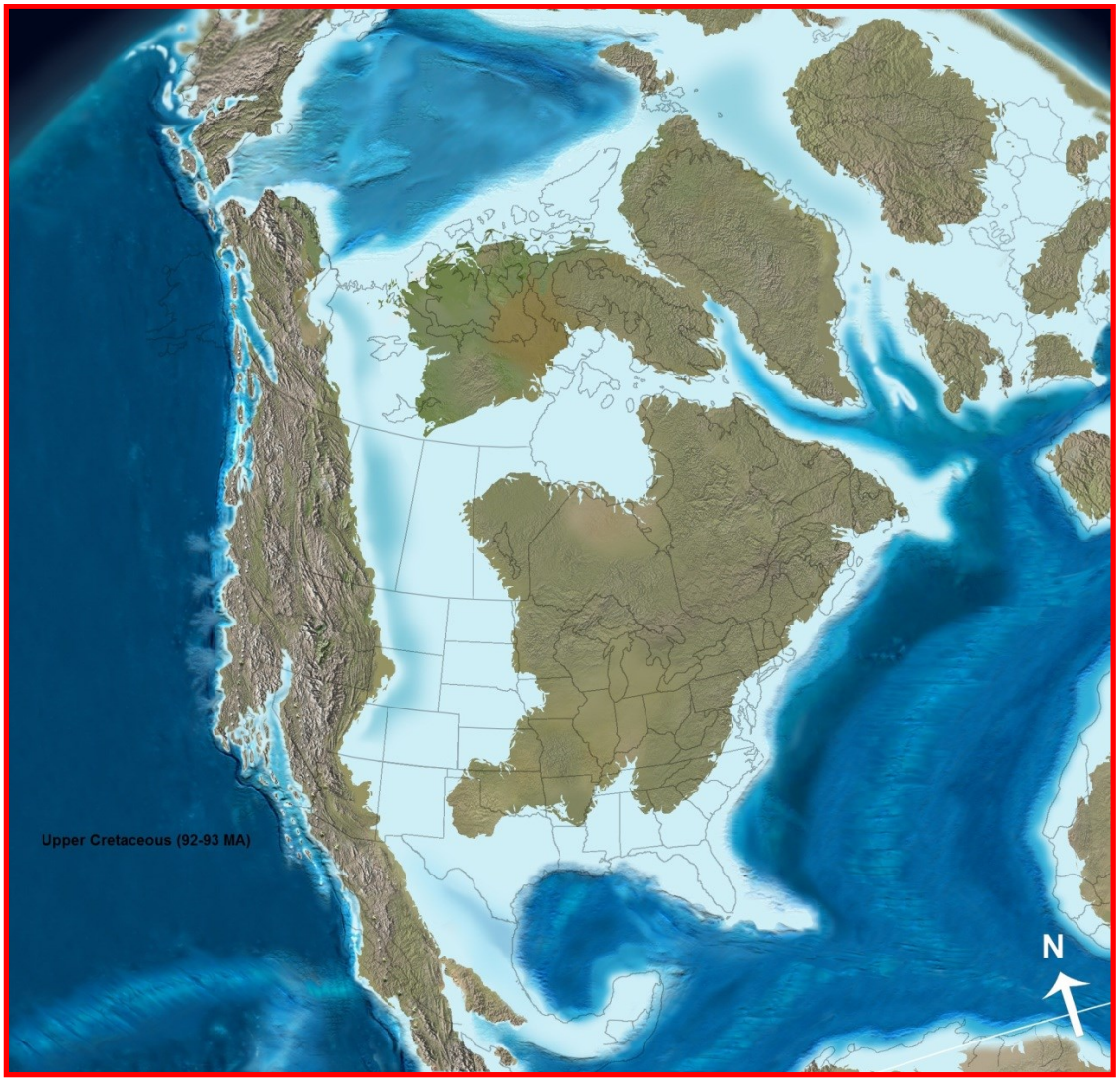

Figure 1. Upper Cretaceous (92-93 MA) paleogeographic map showing the Western Interior Seaway (Image Courtesy of Ron Blakey, NAU Geology).

The cores used for analysis were collected from locations in Central Texas (Travis County, Texas) and South Texas (Frio County, Texas) (**Figure 3**). Core intervals scanned from Travis county, Texas include more complete representations of the rocks deposited before, during, and after OAE 2, as they are continuous cores collected from the Austin Chalk through

the Buda, including the entire Eagle Ford section present in the locale of the core well. The core sample from Frio County, Texas includes a large section of Austin Chalk, but is missing the lower Austin Chalk, upper Eagle Ford, and portions of the lower Eagle Ford. The portion of Buda cored in Frio County, Texas was not scanned, and is therefore not represented.

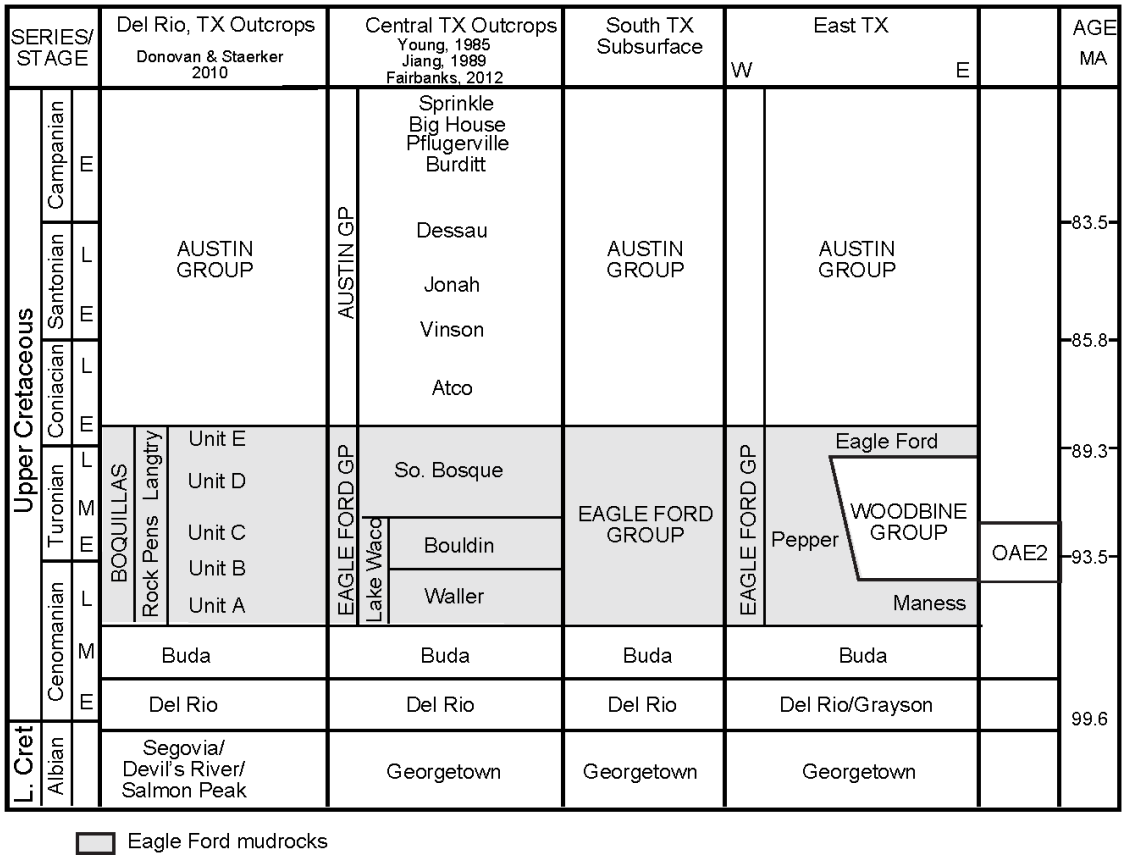

Figure 2. Stratigraphic column of the Eagle Ford and surrounding formations.

1.3 Previous Work

Although no in-depth study has been performed focusing on the geochemistry Eagle Ford, previous studies have been completed which concentrated on rocks of the same age. Hetzel (2009) researched the Demerara Rise off Suriname, South America and Wunstorf, northern Germany. The purpose of the paper was to analyze the geochemistry of sediments

deposited during OAE 2 to determine provenance, degree of anoxia, evaluation of black shale deposition for global TM cycles, and post-depositional element migration. The methodology consisted of XRF analysis of major and trace element concentrations, inductively coupled plasma-mass spectrometry for rare earth elements (REEs), and total organic and inorganic carbon analysis. The Demerara Rise study concluded that the Cretaceous black shales, age equivalent to the Eagle Ford from this study, contained high levels of redox-sensitive and stable sulfide-forming elements as well as a reduction in Mn, indicating reducing conditions during deposition. The Wunstorf study similarly concluded that the Cretaceous black shales contained high levels of redox-sensitive and stable sulfide-forming elements as well as a reduction in Mn, indicating reducing conditions during deposition. Black shale samples from both studies fall into the OAE 2 time interval.

Soua (2011) did a similar study of the Bahloul Formation in Tunisia. The methodology consisted of inductively coupled plasma atomic emission spectroscopy (ICP-AES) and inductively coupled plasma mass spectroscopy to obtain major and trace element concentrations. The purpose of the study was to analyze redox conditions during deposition of the black shales of OAE 2. Based on the analysis of V(V+Ni), Cr/Al, U, V, and Mo, Soua (2011) concluded that the Bahloul Formation was subjected to periodic water bottom euxinia with periods of increased oxygen levels throughout deposition.

1.4 Study Objective

The objective of this study was to use geochemical analysis to aid in the creation of a model of the redox conditions during Eagle Ford deposition. The collection and analysis of XRF data has provided insight as to the specific chemical makeup and the redox conditions of the Eagle Ford compared to the Austin Chalk and Buda. Five cores have been utilized in this study, with emphasis given to the four cores from Travis County, Texas, due to the presence of a more complete geological section. The fifth core, from Frio County, Texas, was missing large

portions of the Eagle Ford, and therefore was not given as much emphasis. The focus of the core analysis was limited to the Eagle Ford (**Figure 2**), sampled at half foot spacing, with secondary focus on the Austin Chalk and Buda, sampled at one to two foot spacing.

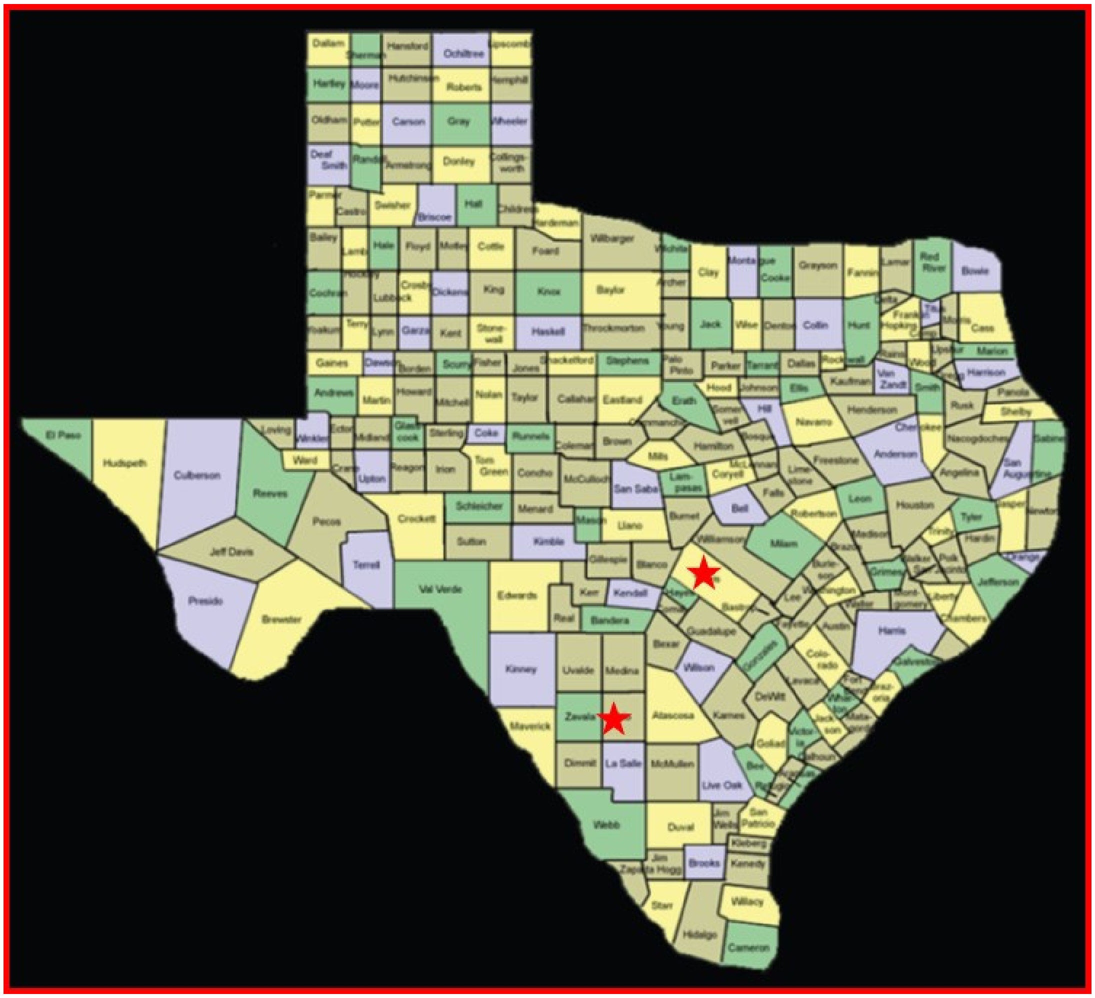

Figure 3. Map showing core locations in Travis County, Texas and Frio County, Texas.

CHAPTER 2

METHODS

2.1 Core Information

Five cores recovered from Texas, four from Central Texas (Travis County) and one core from South Texas (Frio County) preserve sections from the Upper Cretaceous Buda, Eagle Ford, and Austin Chalk (**Table 2.1**). All five cores are currently stored at the Bureau of Economic Geology (BEG) core repository in the J.J. Pickle Research Campus in Austin, Texas. The cores were made available for scanning and review by Dr. Stephen Ruppel, mudrock project activity coordinator at the BEG. The four cores from Travis County, Texas were collected as a part of the Waller Creek Tunnel Project, and the single core from Frio County, Texas was collected from an oil well from the Pearsall Field, which is productive from the Austin Chalk. The significance of the Frio County Calvert core is that the cored interval is currently the target for horizontal wells targeting the Eagle Ford. Core lithologic description was done by Fairbanks, 2012 and presented in **Figure 4**.

Table 2.1 Cores Utilized in Study

Core Name	ACC #1	BO-302 PT	BT-222 PTPZ	BT-221	Calvert #1
Location	Travis County, Texas	Travis County, Texas	Travis County, Texas	Travis County, Texas	Frio County, Texas
(Units)	Feet	Feet	Feet	Feet	Feet
Depth Interval	12.8 - 129.5	26.1 - 99.8	56.5 - 100.2	17.4 - 99.5	5574.4 - 5757.8, 5880.5 - 5943.1, 6115.6 - 6158.9
Length	116.7	73.7	43.7	82.1	289.7
Eagle Ford Interval	80.1 - 124.8	50.9 - 88.3	60.8 - 88.1	51.4 - 87.5	6115.6 - 6158.9
Number of Samples	144	96	43	86	175
Cut Condition	Slabbed	Slabbed	Slabbed	Slabbed	Slabbed

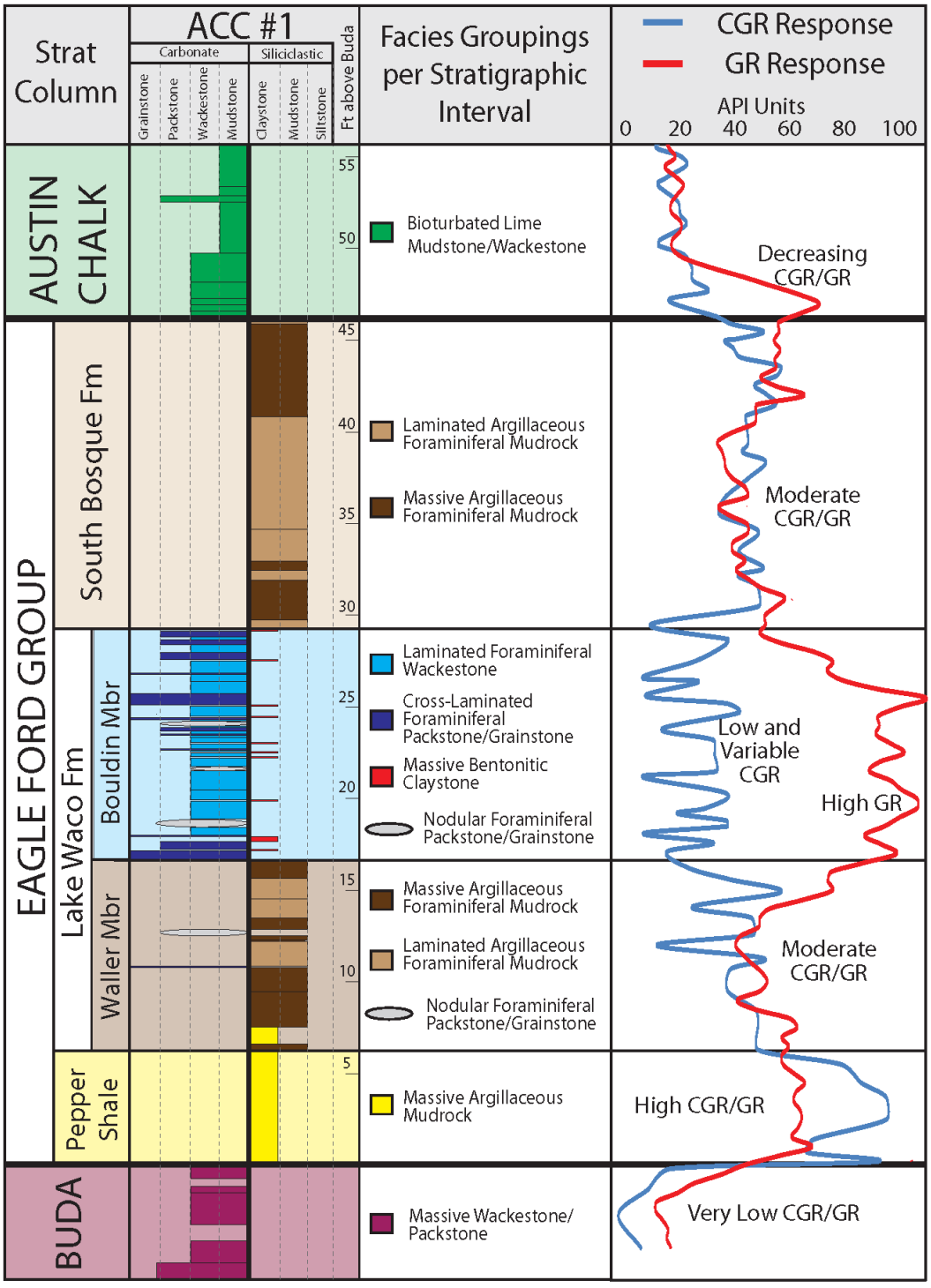

Figure 4. Lithologic description of the Eagle Ford from Travis County, Texas core ACC #1 (Fairbanks, 2012).

2.2 Energy-Dispersive X-Ray Fluorenscence (ED-XRF)

All five cores used in this study were scanned for elemental geochemistry with two different HH-ED-XRF scanners. The Bruker Tracer III-SD, BEG SD3, was utilized for scanning major elements (S, Mg, Cu, P, Si, K, Ca, Ba, Ti, V, Cr, Mn, Fe), while the Bruker Tracer III-V, UTA-2, was utilized for scanning the trace elements (Ni, Cu, Zn, Th, Rb, U, Sr, Y, Zr, Nb, Mo) in each core. The scanners were set up in a stationary way to provide a stable platform for the scanning process. The noses of the instruments were pointed up and the samples were placed on them in such a way as to ensure complete flat surface contact with the instrument (**Figure 5**). Each instrument was supported by a Bruker supplied plastic stabilizing platform accessory. Samples were placed on the noses of the instruments just above a 3 x 4 mm elliptical beam window. Instrument sensitivity decreases by the inverse square of the distance from this window and its subsequent silicon detector (SiPIN), which is found directly beneath the window. In order to obtain the optimal results for each instrument, a flat surface must be used, therefore slabbed core or powdered sample is best, of which slabbed core was utilized.

Major and trace elements were each sampled for 180 seconds, which is the optimal time window for data collection with these instruments. If lithoclasts were found in the core sample to be scanned, the lithoclast was avoided in order to get a more representative reading of the sample of the whole.

Elements which emit K–shell x-rays between 1.25 – 7.06 kV are low–energy spectrum, or major elements. In order to eliminate free air between the emitter in the window, a vacuum pump provided by Bruker was used, with the net result being more accurate major element data. The vacuum reading of 2 μTorr is the maximum allowable reading, but 0 μTorr was observed during data collection, which is optimal.

Elements which emit K-shell x-rays between 6.92 – 19.80 kV are high energy spectrum, or trace elements. A Cu–Ti–Al filter was inserted between the detector and sample window to

filter out low-energy x-rays, keeping them from interfering with the high-energy x-rays. The net result was the emission of x-rays at 40 kV and 28 μA.

Figure 5. Setup of HH-ED-XRF showing laptop for collecting data from the scanner, a core sample resting on the nose of the instrument, the scanner (BEG-SD3), and the vacuum pump (partially obscured by a PVC pipe) scanning a core sample for major element analysis.

2.3 ED-XRF Mudrock Calibration

Calibration of the raw data procured by the ED-XRF is necessary in order to convert to usable data in the form of quantitative percentages for the major elements and estimated parts per million (ppm) for the trace elements. The calibration was developed utilizing five commercially available standards and eighty-five in-house reference materials (Rowe, Hughes, Robinson, 2012). The 90 reference materials are sourced as follows: 5 international, 7 Devonian-Mississippian Ohio Shale, 20 Pennsylvanian Smithwick Formation from Central

Texas, 27 Devonian-Mississippian Woodford Formation from West Texas, 15 Upper Cretaceous Eagle Ford Formation from South Texas, and 16 Mississippian Barnett Formation from North-Central Texas.

Each of the 90 samples was pulverized to 200 mesh using a TM Engineering Pulverizer equipped with trace-metal grade grinding barrels. Using a Carver press to 40 tons with a 40 mm die, roughly 8 grams of each powdered sample was pressed to a borate-fused disc. The reference pellets were then analyzed for major and trace elements using wavelength-dispersive x-ray fluorescence (WD-XRF) and inductively-coupled plasma mass spectrometry (ICP-MS), respectively (Hughes, 2011).

Bruker used an ED-XRF to obtain the data for the standards and entered it into their software package in order to complete the calibration process for the ED-XRF. Rousseau (2001) provided a table for the lowest detectable measurements (**Table 2.2**).

2.4 Geochemical Overview

The application of geochemical proxies in determination of depositional redox conditions is regarded as a reliable methodology (Jones and Manning, 1994; Tribovillard, Algeo, Baudin, Riboulleau, 2011). Trace metal (TM) concentrations in different redox conditions have been compared to generate consistent models used to understand paleoenvironmental depositional conditions (Brumsack, 1989). Before any conclusions are drawn from TM concentrations, it is important to understand the paleogeological setting from which the analyzed samples were collected. The three major settings include the a) unrestricted upwelling zone, b) weakly restricted silled basin, and c) the strongly restricted silled basin (Algeo and Rowe, 2011). **Figure 6** graphically illustrates the three major geological depositional settings. The setting also influences concentrations of major elements such as Mn (Algeo and Lyons, 2006). Since Mn becomes mobile in reducing conditions, in an unrestricted setting, it may be removed from the oxygen minimum zone (OMZ) and will therefore be found in lower concentrations. This setting is easy to recognize reducing conditions from low Mn levels. A

weakly restricted setting may be slightly more difficult to recognize, as the Mn may not have been removed to the degree it was in the unrestricted setting. The strong restriction setting would be the most difficult to recognize with Mn concentrations, as the Mn would be made mobile by the reducing conditions, but is not removed from the system. A general reduction in TM concentrations is expected due to lack of deepwater renewal.

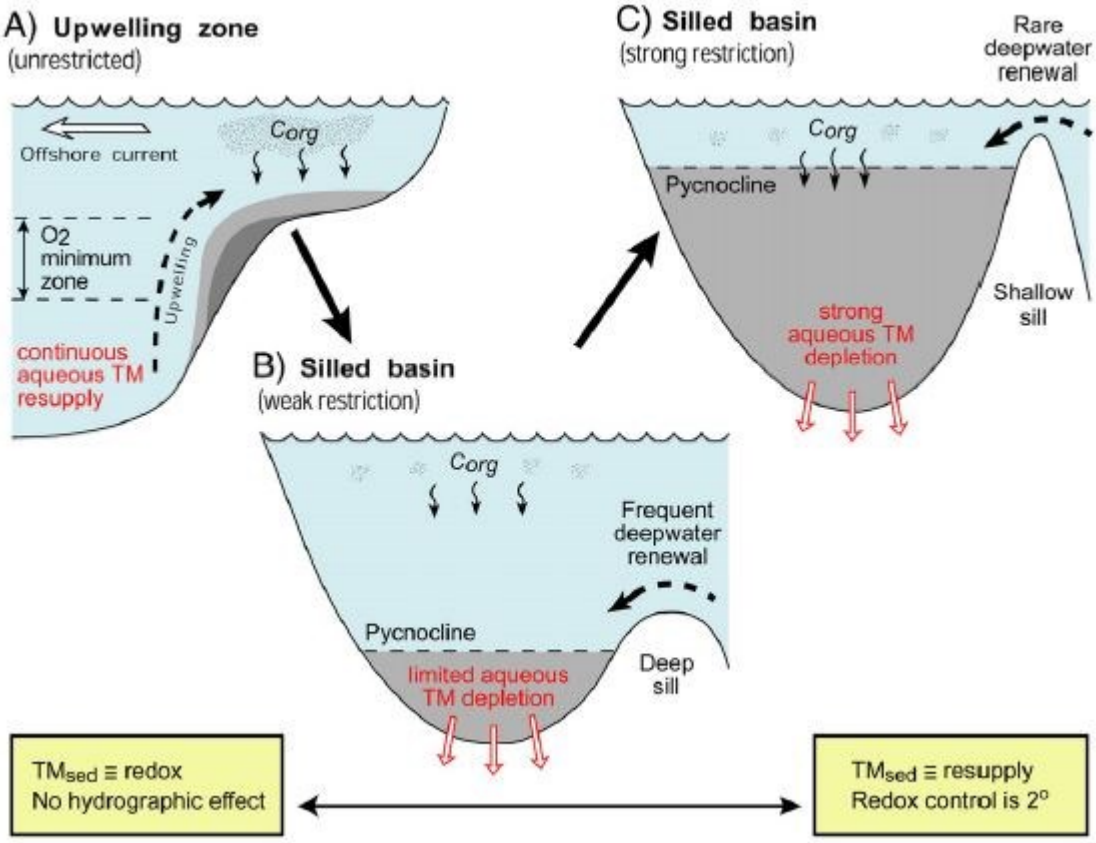

Figure 6. Three major geological depositional settings from Algeo and Rowe (2011). Each setting represents different degrees of deepwater renewal, influencing TM concentrations.

2.5 Geochemical Proxies

2.5.1 Paleo-oxygenation Proxies

Tribovillard, Algeo, Lyons, and Riboulleau (2006) listed a fairly comprehensive index of paleo-oxygenation elemental proxies. The main elements identified include U, V, and Mo. Each

of these three elements have been shown to increase in accumulation rates as the bottom water moves from oxic to reducing conditions (Algeo and Maynard, 2004). Mn plays an important role in the transport of these three elements through the water column, but is not cited as specifically being a reliable indicator of explicit redox conditions (Tribovillard et al, 2006; Calvert and Pedersen, 1993). The role of Mn begins in more oxic conditions, where it typically exists as an oxyhydroxide. Immobile as an oxyhydroxide, Mn may host trace metals which adsorb to it in the more oxygen-rich water (Collier, 1985; Koide, Hodge, Tang, Stallard, Goldberg, Calhoun, Bertine, 1986; Colodner, Sachs, Ravizza, Turekian, Edmont, Boyle, 1993; Turgeon and Brumsack, 2006). As the Mn oxyhydroxides with trace metal adsorbed travel into more reducing bottom water, reductive dissolution begins to break apart the now mobile Mn compounds, releasing free Mn back into the water column, leaving the once adsorbed trace metals deposited at the sediment surface as sulfides or organo-metallic compounds, such as porphyrins (Simoneit, 1978; Kremling, 1983; Jacobs, Emerson, Skei, 1985; Tribovillard et al., 2006). The net effect of the above described process is the enrichment of the trace metals U, V, and Mo, and an overall decrease in Mn.

2.5.2 Organic Matter (OM) Proxies

Ba and P have been put forward as productivity indices (Goldberg and Arrhenius, 1958; Dehairs, Chesselet, Jedwab, 1980; Schmitz, 1987; Lea and Boyle, 1990; Dymond, Suess, Lyle, 1992; Turgeon and Brumsack, 2006). Tribovillard (2006) posited that Cu and Ni were acceptable proxies for the deposition of OM. Cu and Ni are easily bound by settling organic particles, providing the pathway for distribution in the sediment. The presence of abundant Cu and Ni in the strata indicates that high volumes of OM must have been present to transport them to the sediment where reducing conditions allowed their fixation within the sediment. Pyrite is the major mineral to which they tend to become affixed under such conditions. It is this

tendency of Cu and Ni to bind to pyrite which leads to storage within the sediment that makes them better OM proxies than P and Ba.

Table 2.2. Lowest Detectable Measurements for XRF Scanners

Element	Accepted Value[a]	Instrument 1 (UTA-1) Measured Value[b]	σ (n=7)[b]	LDM[c]	Instrument 2 (1st UTA-2) Measured Value[b]	σ (n=7)[b]	LDM[c]
Mg (%)	0.67	0.80	0.09	0.17	0.85	0.14	0.28
Al (%)	4.96	5.39	0.14	0.28	5.32	0.11	0.22
Si (%)	32.6	33.7	0.2	0.5	33.1	0.4	0.8
P (%)	0.07	0.05	0.03	0.07	0.09	0.03	0.06
S (%)	3.34	2.18	0.10	0.20	2.27	0.09	0.18
K (%)	2.07	2.31	0.09	0.18	2.22	0.07	0.14
Ca (%)	0.13	0.23	0.03	0.06	0.24	0.02	0.04
Ti (%)	0.23	0.27	0.02	0.04	0.27	0.02	0.03
Mn (%)	0.015	0.012	0.001	0.002	0.013	0.001	0.003
Fe (%)	2.93	2.55	0.06	0.12	2.52	0.06	0.13
Ba (ppm)	2090	1884	376	753	1700	300	600
V (ppm)	928	1114	68	137	1110	80	159
Cr (ppm)	110	98	13	26	106	14	27
Ni (ppm)	130	153	26	52	150	20	40
Cu (ppm)	83	147	20	40	87	12	23
Zn (ppm)	823	844	96	191	880	74	147
Th (ppm)	8.4	9	1	2	9	1	2
Rb (ppm)	122	123	12	25	131	12	25
U (ppm)	18.1	17	6	11	22	4	8
Sr (ppm)	75.5	87	5	10	93	9	18
Y (ppm)	35.4	34	3	5	36	2	4
Zr (ppm)	80.3	95	7	13	96	6	13
Nb (ppm)	9	9	1	2	9	1	2
Mo (ppm)	79	83	4	9	82	3	6

A - Values for major elements from lithium borate-fused disc analysis by WD-XRF at SGS; values for trace elements (ppm) from sodium borate fusion dissolution and analysis by ICP-MS.

B - Average HH-ED-XRF measured values (n = 7) and standard deviations (s) for reference material RTC-W-260, a black shale from the Devonian Woodford Formation of West Texas.

C - Limit of Determination of a Method (LDM) calculated according to Rousseau

CHAPTER 3

RESULTS

3.1 Data Overview

A detailed stratigraphic description of the Eagle Ford by Fairbanks (2012) provided the parameters used in this study (**Figure 4**). Results from the geochemical data are presented graphically to illustrate both local and regional changes in the Eagle Ford. Readings were taken on a predefined interval of one to two feet between sample for the Austin Chalk, above the Eagle Ford, and for the Buda, below the Eagle Ford. The sample for the Eagle Ford sections was set at half-foot intervals in order to achieve higher resolution. All samples were chosen to exclude any clasts or other features which did not represent the sampled interval as a whole. Results for all cores included in this study were presented as a comparison of the Eagle Ford to the Austin Chalk above and Buda below, with the exception of the Calvert core from Frio County, which did not include a complete section of any of the aforementioned stratigraphic layers.

The XRF data collected have been compiled into graphs representing various geochemical ratios based on elemental concentrations. Three types of graphs utilized include two variable scatter plots, three variable ternary diagrams, and multiple variable graphs plotted against depth.

The two variable scatter plots were specifically used to determine direct relationships between two elements. This is helpful in identifying the likely mineralogy from which the element in question is bound. An example of this is Al plotted against Si to determine if the Si was bound in clays or siliciclastics. With the absence of direct mineral speciation, which may be provided by XRD analysis, these plots represent a much broader, but still effective, mineralogy.

The three variable ternary diagram plots Si versus Al versus Ca. Plotting these three elements against each other in a ternary diagram graphically represents the geochemical lithology of each sample entered. The Si is representative of SiO_2, or siliciclastics. The Al is

representative of AL_20_3, or clays. The Ca is representative of CaO, or carbonates. The average gray shale as defined by Wedepohl (1971) is plotted on the ternary diagram to be used as a graphical comparison of the plotted samples.

The multiple variable graphs plotted against depth are useful for comparing elemental concentrations from the same depth interval. If at a specific depth reducing conditions are suspected, a direct comparison among redox sensitive elements may be readily observed, where the suspicions may be verified or dismissed.

Figure 7 shows the breakdown of colors used to represent the Austin Chalk, Eagle Ford, and Buda. The same color scheme is used in all plots and graphs to easily discern the different horizons.

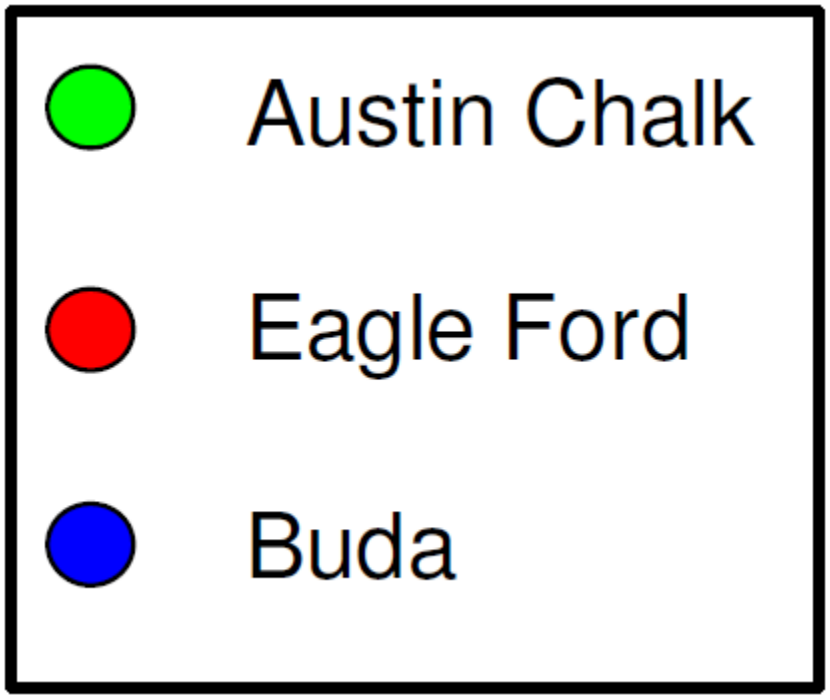

Figure 7. Color Scheme used in all plots and graphs.

3.2 Major Element Analysis

Major elemental analysis and quantification were used to determine the chief lithologies of the Austin Chalk, Eagle Ford, and Buda, with the main focus on the Eagle Ford. The Austin

Chalk and Buda maintain very high levels of calcium carbonate while the Eagle Ford rocks vary is calcium carbonate levels as you move from more calcium carbonate rich South Texas over the San Marcos Arch into East Texas, where they tend to become more siliciclastic shales. **Figures 8, 12, 16, 20, 24** are ternary diagrams representing the various lithologies.

Al, as the geochemical proxy for clay, has been used to make cross plots against other major elements in order to determine the mineral phase in which the given element exists in each sample. When a strong correlation between Al and the major element plotted against it was noticed, it was determined that the element likely existed in a clay mineral phase. **Figures 10, 14, 18, 22, 26** represent major elements plotted versus Al in each core studied. A significant observation is the linear relationship between Si and Al, indicating a lack of siliciclastic influx during the deposition of Eagle Ford strata in Central Texas (Travis County). This means that, most likely, any Si present in the Eagle Ford is present in the clay mineral phase. The Si does show slight enrichment versus Al in the Calvert core, which may be indicative of a very minor influence of siliciclastics in South Texas Eagle Ford. It should be noted that the amount of Eagle Ford cored and scanned in the Calvert is less than half of the entire Eagle Ford section, and is not representative of the Eagle Ford as a whole. Ideally, the entire Eagle Ford section would have been cored and scanned, and in more than one well, in order to gain a more representative sample of South Texas Eagle Ford. **Figures 9, 13, 17, 21, 25** isolate Ca versus Al to clarify the carbonate-richness of the Eagle Ford strata.

Ca, as the geochemical proxy for calcium carbonate, has been used to make cross plots against other major elements in order to determine the relationship among calcium carbonate and the other major elements by identifying linear trends. Fe, when found in higher concentrations of Ca, may represent the mineral phase siderite, whereas Mg found with higher levels of Ca may represent the mineral phase of dolomite. **Figures 11, 15, 19, 23, 27** represent cross plots of major elements versus Ca.

3.2.1 ACC 1 Core

Lithologies of the Austin Chalk and Buda cluster in the carbonate corner of the ternary diagram, indicating very little sourcing other than carbonates (**Figure 8**). The Ca/Al plot illustrates a very linear relationship between the two elements, with most plotted points falling in the high Ca, low Al section (**Figure 9**). This has been interpreted as occasional clay deposition in a predominantly carbonate setting for both the Austin Chalk and Buda. **Figure 10** shows Mn/Al values for the Austin Chalk and Buda, which indicate Mn enrichment associated with low Al values. Mn/Ca values indicate Mn enrichment associated with higher levels of Ca (**Figure 11).** This has been interpreted as oxic conditions dominating during Austin Chalk and Buda deposition.

The Eagle Ford lithologies follow a very linear line from the carbonate corner of the ternary diagram to the average gray shale point, as defined by Wedepohl (1971). This was interpreted as dominantly carbonate-rich shale which occasionally grades to the level of the average gray shale. This interpretation was strengthened by the Ca/Al plot, showing the Eagle Ford following a linear relationship between the two elements. The Mn/Al plot shows a marked decrease in Mn as Al levels rose. Most Eagle Ford points plotted fell into higher Al values where Mn was greatly reduced. This has been interpreted as anoxic conditions prevailing during much of the deposition of the Eagle Ford.

Several small instances of increased Ca were noted in the central portion of the Eagle Ford. Associated with these Ca-rich streaks were increased Mn values. These streaks have been interpreted as minor periods during Eagle Ford deposition where conditions became oxic, allowing Mn to remain fixed as oxy/hydroxides in the sediment.

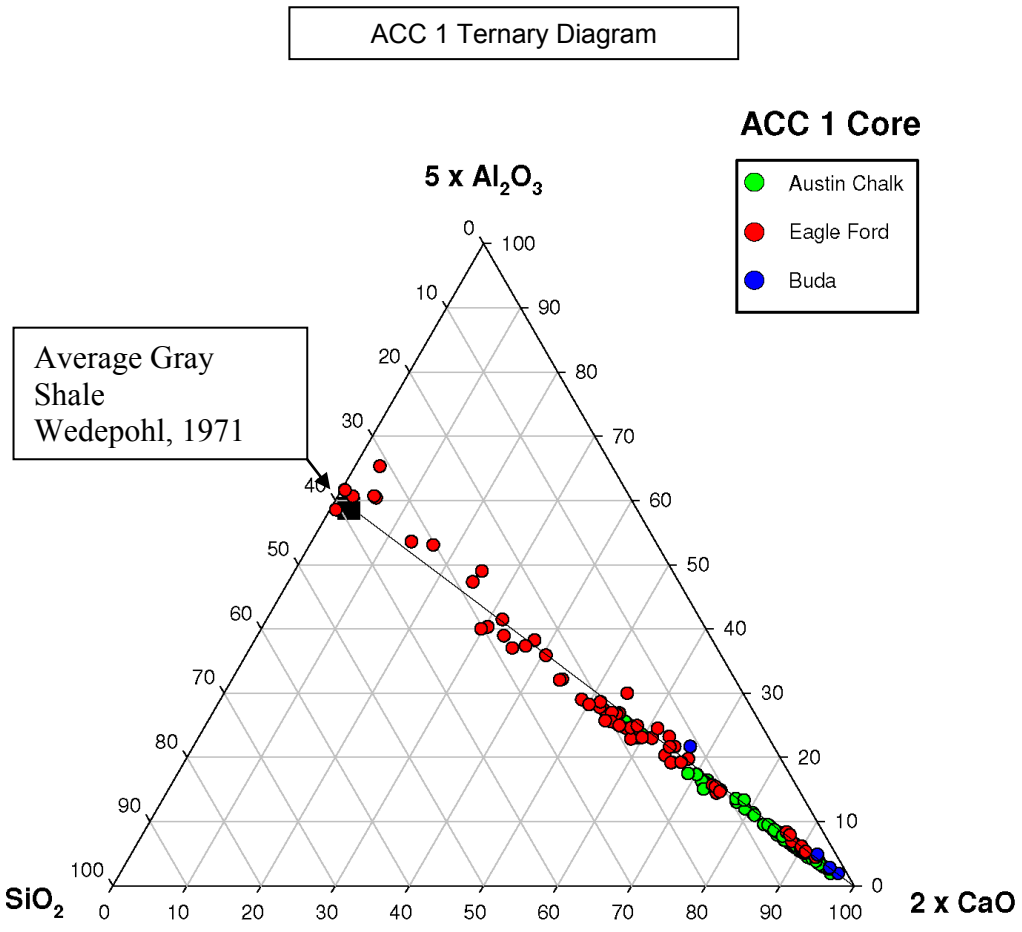

Figure 8. Ternary diagram representing the lithologies of the Austin Chalk, Eagle Ford, and Buda in the ACC 1 core, Travis County, Texas.

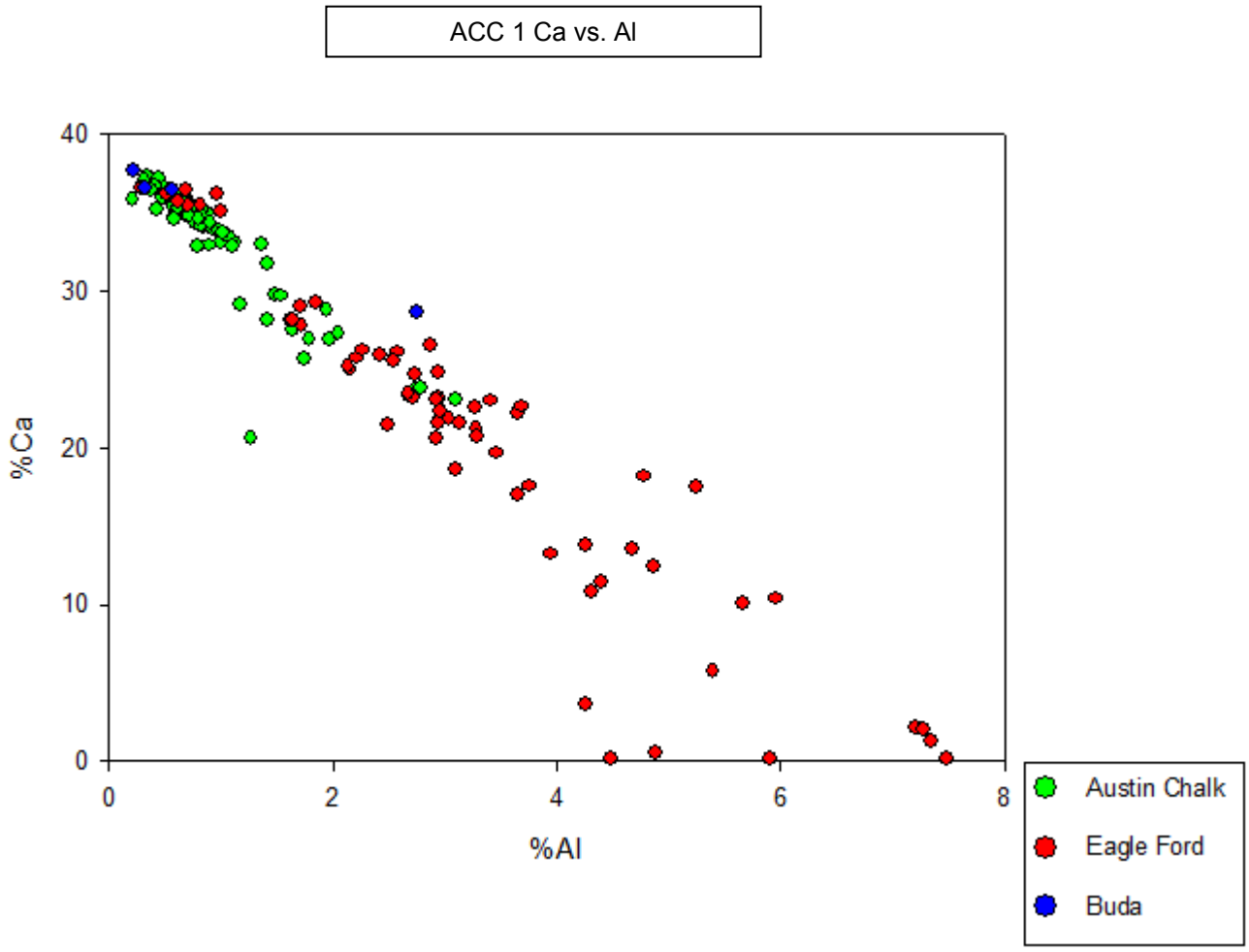

Figure 9. Carbonate richness versus clay in the ACC 1 core.

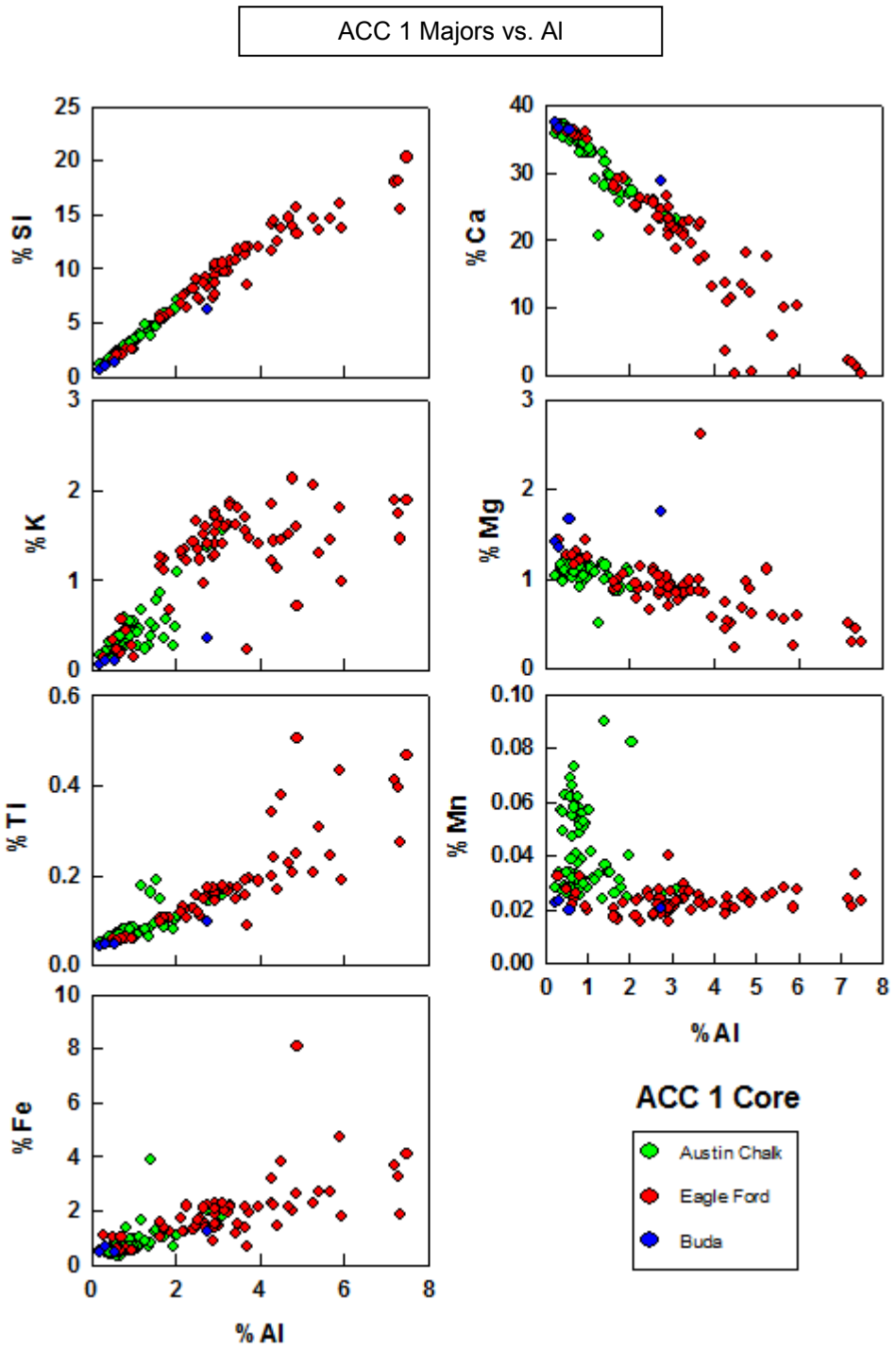

Figure 10. Major elements plotted against Al to qualify clay versus non-clay phase mineral abundances of each element in the ACC 1 core.

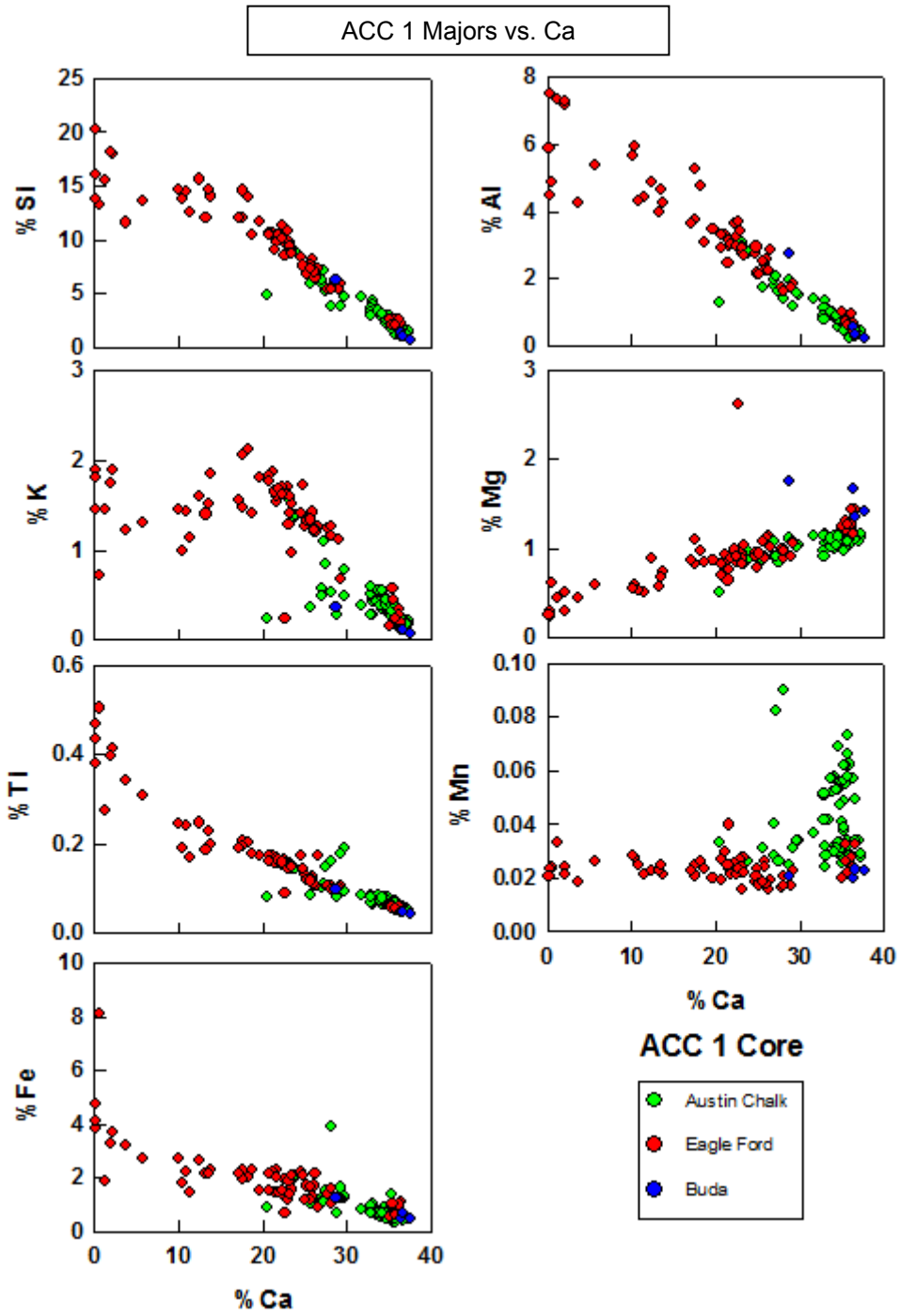

Figure 11. Major elements plotted against Ca to qualify carbonate mineral abundances of each element in the ACC 1 core.

3.2.2 BT 221 Core

Lithologies of the Austin Chalk and Buda cluster in the carbonate corner of the ternary diagram, indicating very little sourcing other than carbonates (**Figure 12**). The Ca/Al plot in **figure 13** illustrates a very linear relationship between the two elements, with most plotted points falling in the high Ca, low Al section. This has been interpreted as occasional clay deposition in a predominantly carbonate setting for both the Austin Chalk and Buda. Mn/Al values for the Austin Chalk and Buda indicate Mn enrichment associated with low Al values (**Figure 14**). Mn/Ca values indicate Mn enrichment associated with higher levels of Ca (**Figure 15**). This has been interpreted as oxic conditions dominating during Austin Chalk and Buda deposition.

The Eagle Ford lithologies follow a very linear line from the carbonate corner of the ternary diagram to the average gray shale point, as defined by Wedepohl (1971). This was interpreted as dominantly carbonate-rich shale which occasionally grades to the level of the average gray shale. This interpretation was strengthened by the Ca/Al plot, showing the Eagle Ford following a linear relationship between the two elements. The Mn/Al plot shows a marked decrease in Mn as Al levels rose. Most Eagle Ford points plotted fell into higher Al values where Mn was greatly reduced. This has been interpreted as anoxic conditions prevailing during much of the deposition of the Eagle Ford.

Three streaks of increased Ca were noted in the central portion of the Eagle Ford. Associated with these Ca-rich streaks were increased Mn values. These streaks have been interpreted as minor periods during Eagle Ford deposition where conditions became oxic, allowing Mn to remain fixed as oxy/hydroxides in the sediment.

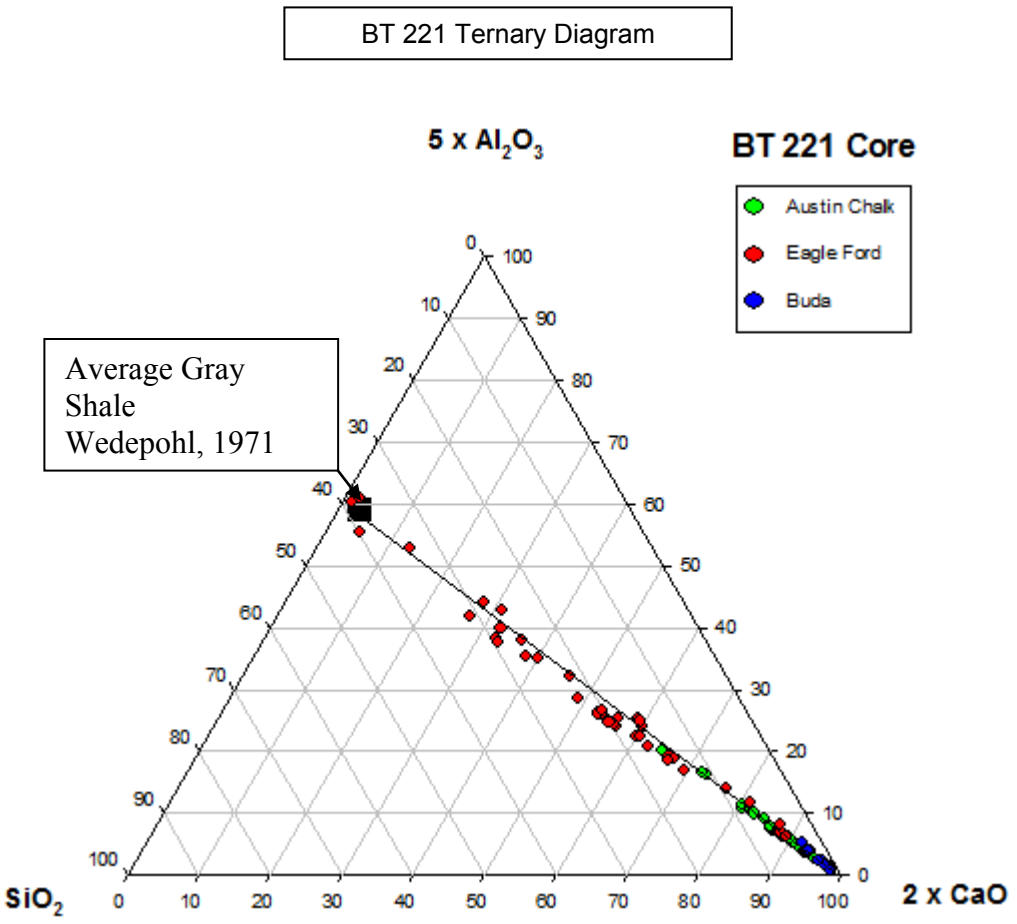

Figure 12. Ternary diagram representing the lithologies of the Austin Chalk, Eagle Ford, and Buda in the BT 221 core, Travis County, Texas.

BT 221 Ca vs. Al

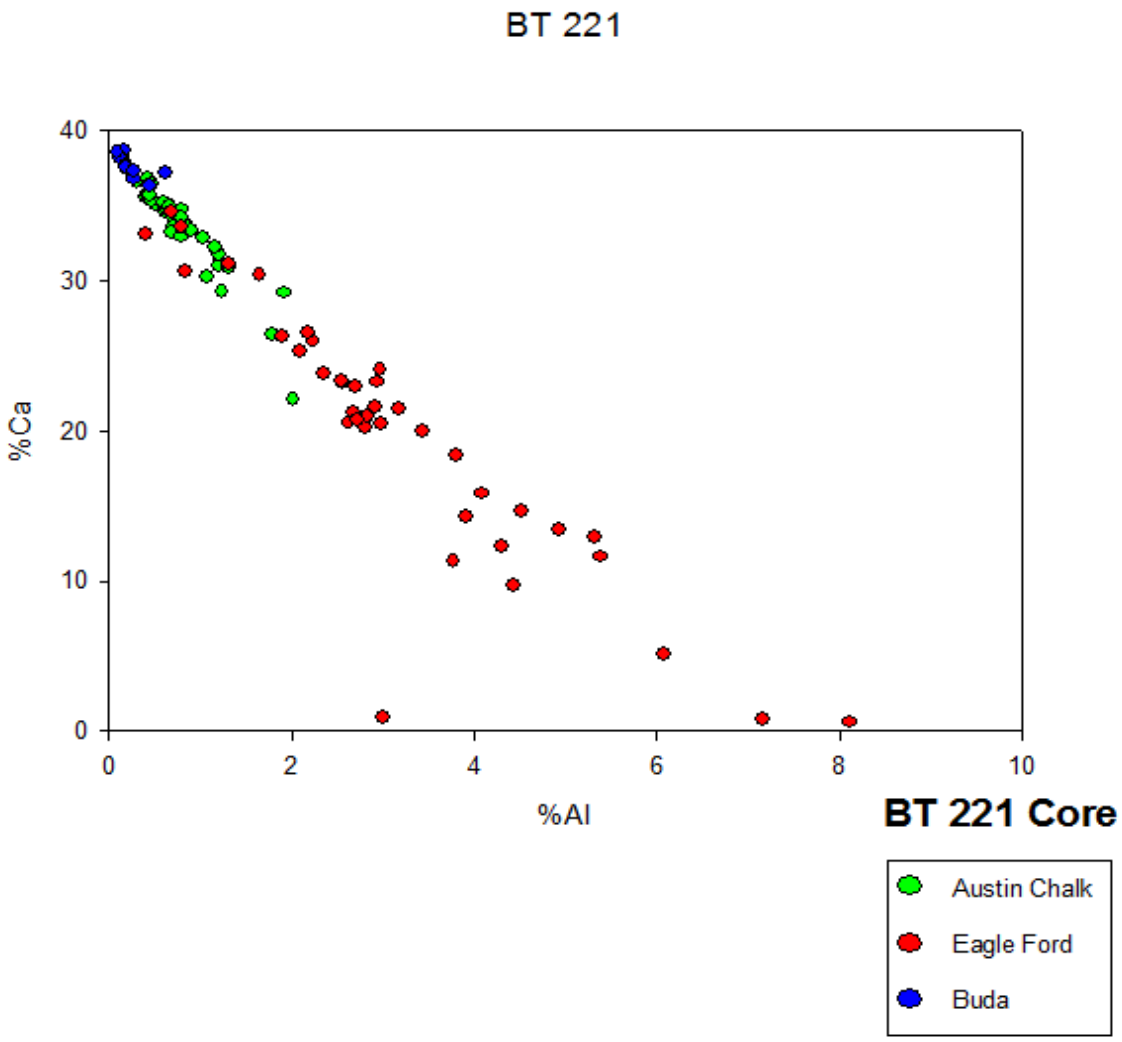

Figure 13. Carbonate richness versus clay in the BT 221 core.

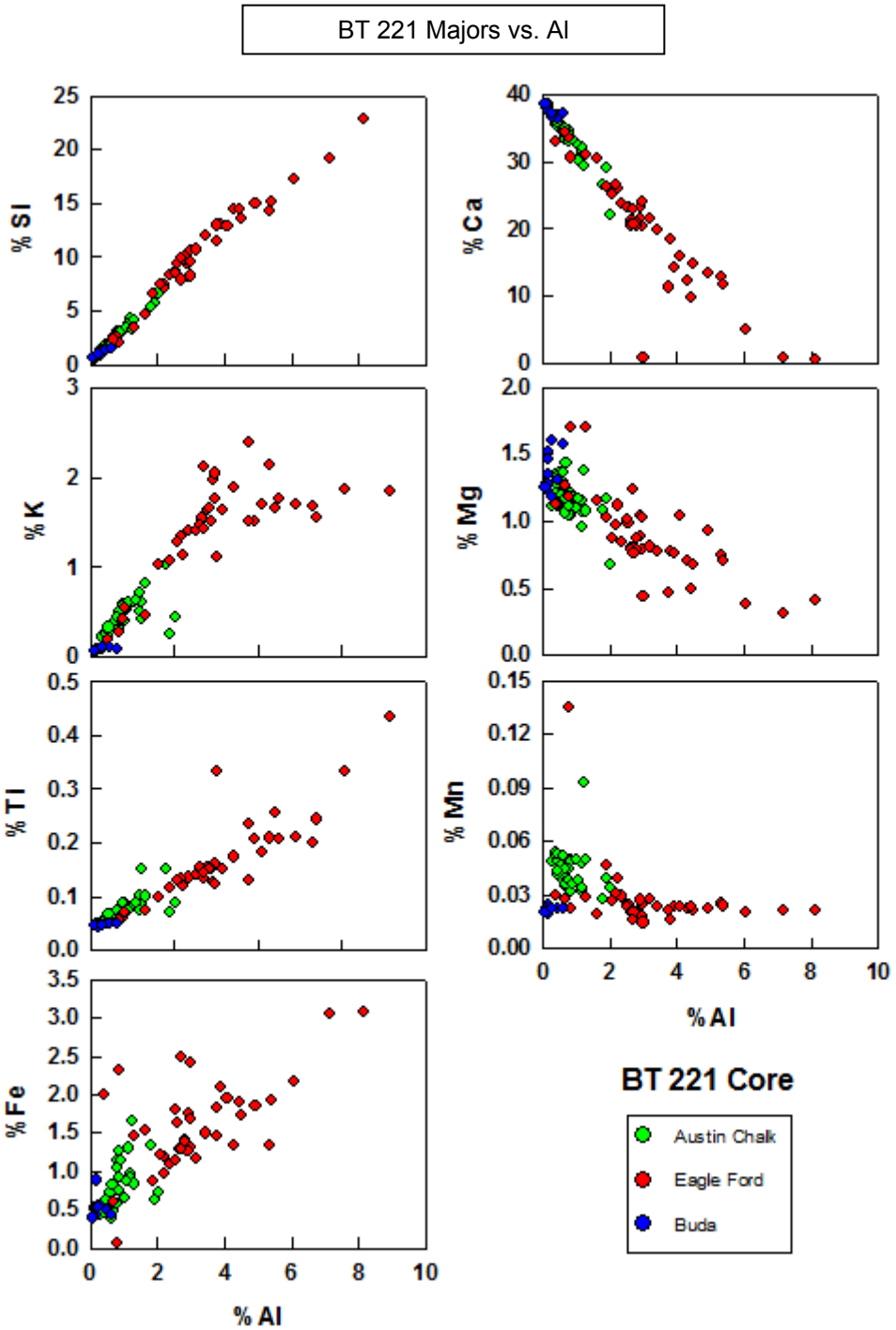

Figure 14. Major elements plotted against Al to qualify clay versus non-clay phase mineral abundances of each element in the BT 221 core.

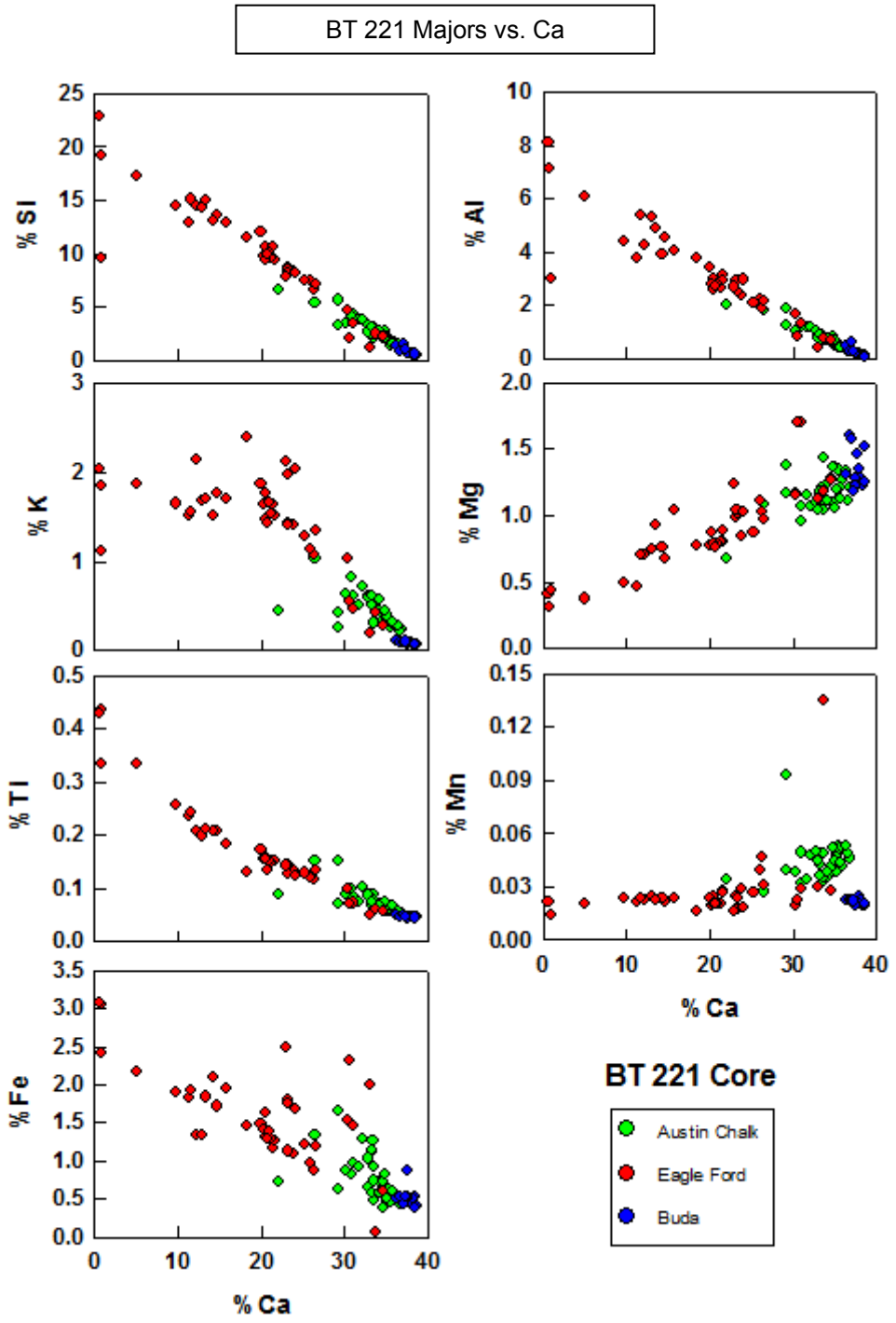

Figure 15. Major elements plotted against Ca to qualify carbonate mineral abundances of each element in the BT 221 core.

3.2.3 BT-222 Core

Lithologies of the Austin Chalk and Buda cluster in the carbonate corner of the ternary diagram, indicating very little sourcing other than carbonates (**Figure 16**). The Ca/Al plot illustrates a very linear relationship between the two elements, with most plotted points falling in the high Ca, low Al section (**Figure 17**). This has been interpreted as occasional clay deposition in a predominantly carbonate setting for both the Austin Chalk and Buda. Mn/Al values for the Austin Chalk and Buda indicate Mn enrichment associated with low Al values (**Figure 18**). Mn/Ca values indicate Mn enrichment associated with higher levels of Ca (**Figure 19**). This has been interpreted as oxic conditions dominating during Austin Chalk and Buda deposition.

The Eagle Ford lithologies follow a very linear line from the carbonate corner of the ternary diagram to the average gray shale point, as defined by Wedepohl (1971). This was interpreted as dominantly carbonate-rich shale which occasionally grades to the level of the average gray shale. This interpretation was strengthened by the Ca/Al plot, showing the Eagle Ford following a linear relationship between the two elements. The Mn/Al plot shows a marked decrease in Mn as Al levels rose. Most Eagle Ford points plotted fell into higher Al values where Mn was greatly reduced. This has been interpreted as anoxic conditions prevailing during much of the deposition of the Eagle Ford.

Two small streaks of increased Ca were noted in the central to upper portion of the Eagle Ford. Associated with these Ca-rich streaks were increased Mn values. These streaks have been interpreted as minor periods during Eagle Ford deposition where conditions became oxic, allowing Mn to remain fixed as oxy/hydroxides in the sediment.

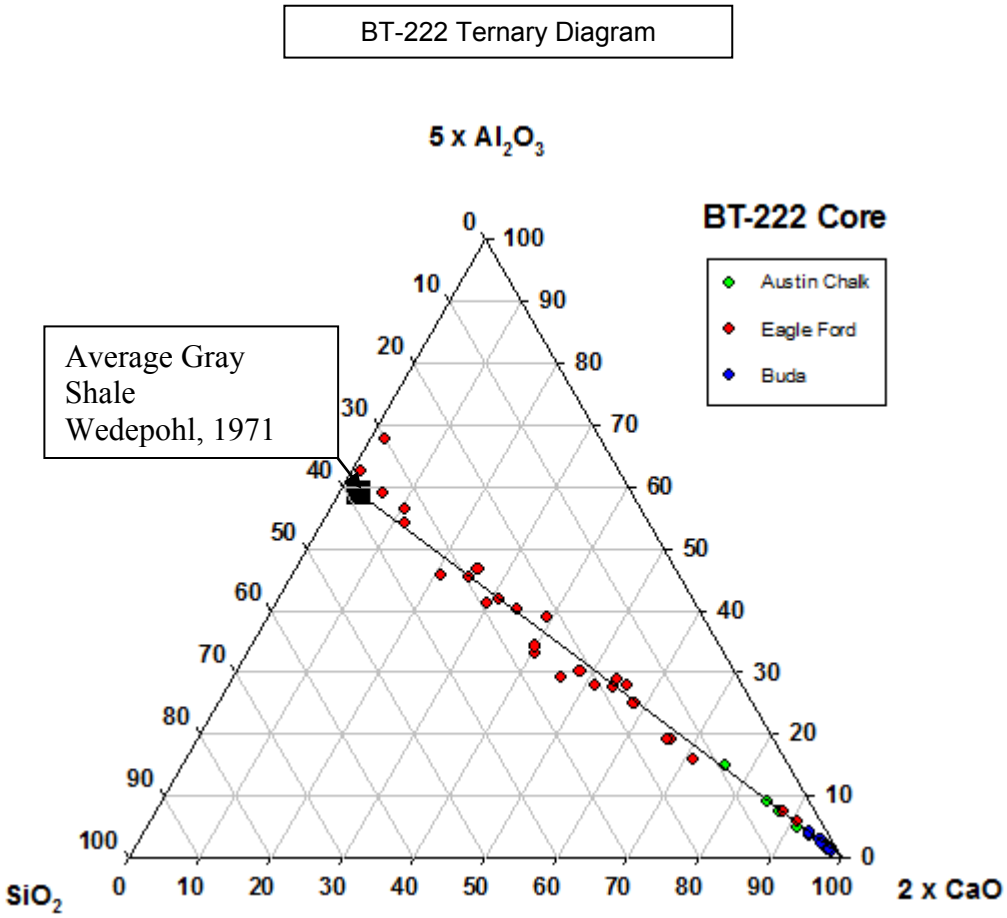

Figure 16. Ternary diagram representing the lithologies of the Austin Chalk, Eagle Ford, and Buda in the BT-222 core, Travis County, Texas.

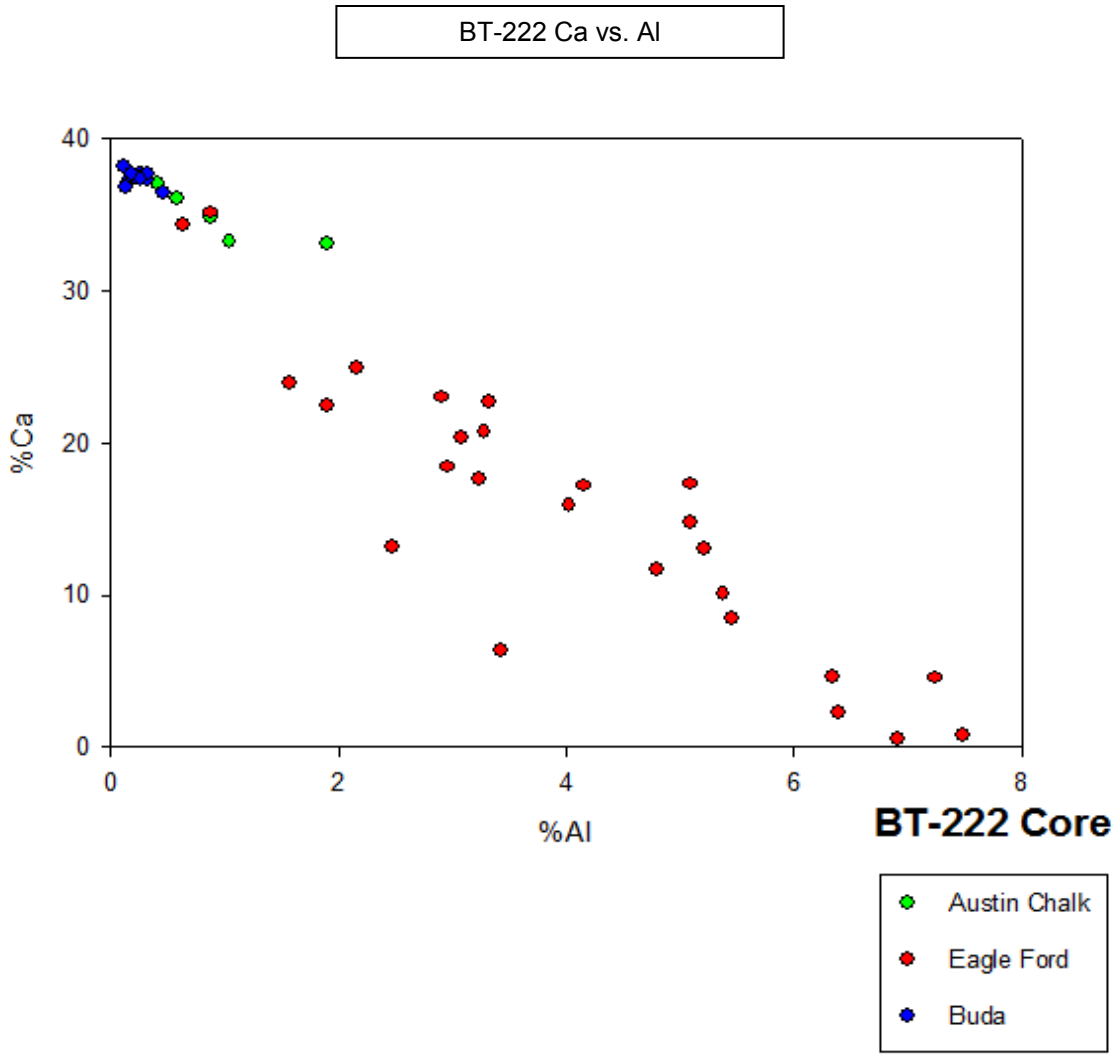

Figure 17. Carbonate richness versus clay in the BT-222 core.

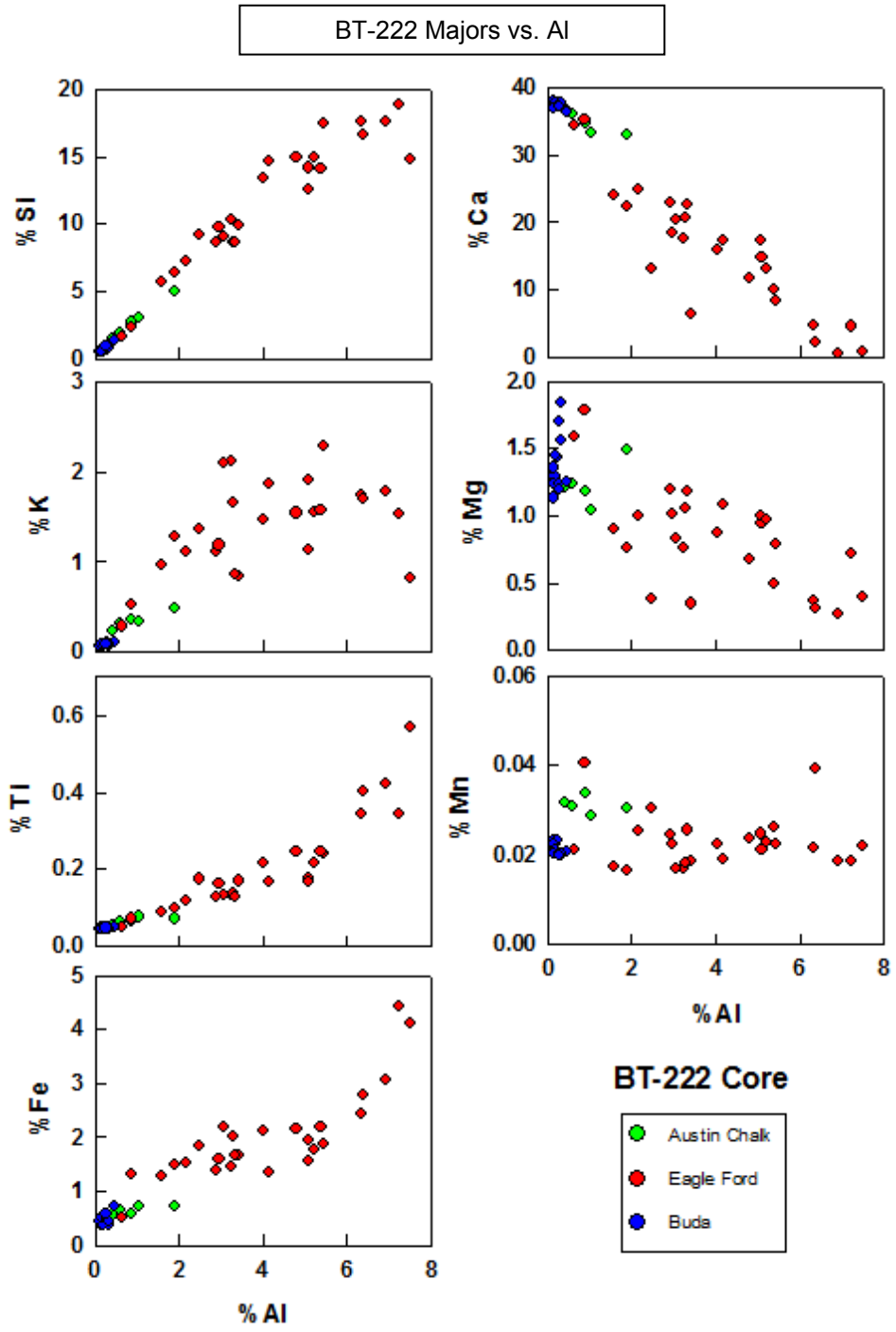

Figure 18. Major elements plotted against Al to qualify clay versus non-clay phase mineral abundances of each element in the BT-222 core.

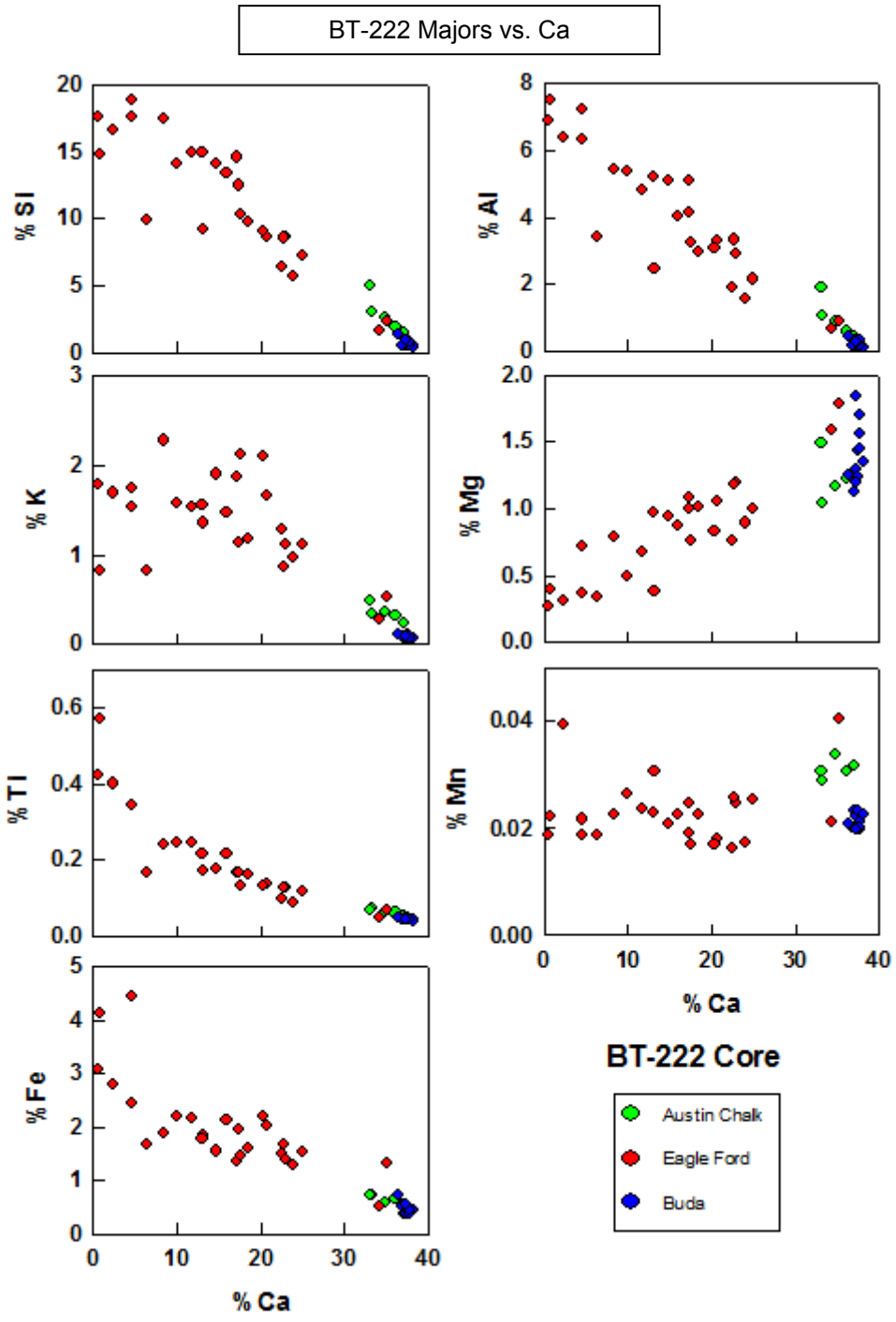

Figure 19. Major elements plotted against Ca to qualify carbonate mineral abundances of each element in the BT-222 core.

3.2.4 BO 302 PT Core

Lithologies of the Austin Chalk and Buda cluster in the carbonate corner of the ternary diagram, indicating very little sourcing other than carbonates (**Figure 20**). The Ca/Al plot illustrates a very linear relationship between the two elements, with most plotted points falling in the high Ca, low Al section (**Figure 21**). This has been interpreted as occasional clay deposition in a predominantly carbonate setting for both the Austin Chalk and Buda. Mn/Al values for the Austin Chalk and Buda indicate Mn enrichment associated with low Al values (**Figure 22**). Mn/Ca values indicate Mn enrichment associated with higher levels of Ca (**Figure 23**). This has been interpreted as oxic conditions dominating during Austin Chalk and Buda deposition.

The Eagle Ford lithologies follow a very linear line from the carbonate corner of the ternary diagram to the average gray shale point, as defined by Wedepohl (1971). This was interpreted as dominantly carbonate-rich shale which occasionally grades to the level of the average gray shale. This interpretation was strengthened by the Ca/Al plot, showing the Eagle Ford following a linear relationship between the two elements. The Mn/Al plot shows a marked decrease in Mn as Al levels rose. Most Eagle Ford points plotted fell into higher Al values where Mn was greatly reduced. This has been interpreted as anoxic conditions prevailing during much of the deposition of the Eagle Ford.

Three small streaks of increased Ca were noted in the central portion of the Eagle Ford. Associated with these Ca-rich streaks were increased Mn values. These streaks have been interpreted as minor periods during Eagle Ford deposition where conditions became oxic, allowing Mn to remain fixed as oxy/hydroxides in the sediment.

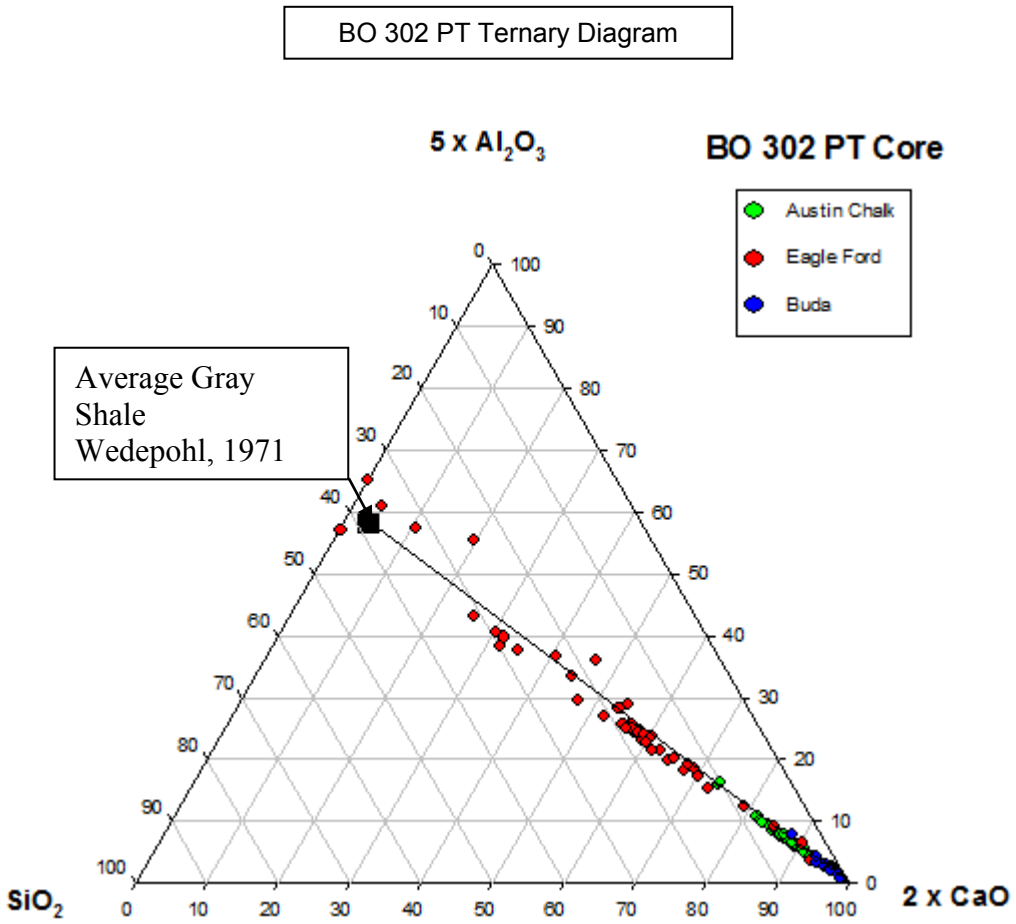

Figure 20. Ternary diagram representing the lithologies of the Austin Chalk, Eagle Ford, and Buda in the BO 302 PT core, Travis County, Texas.

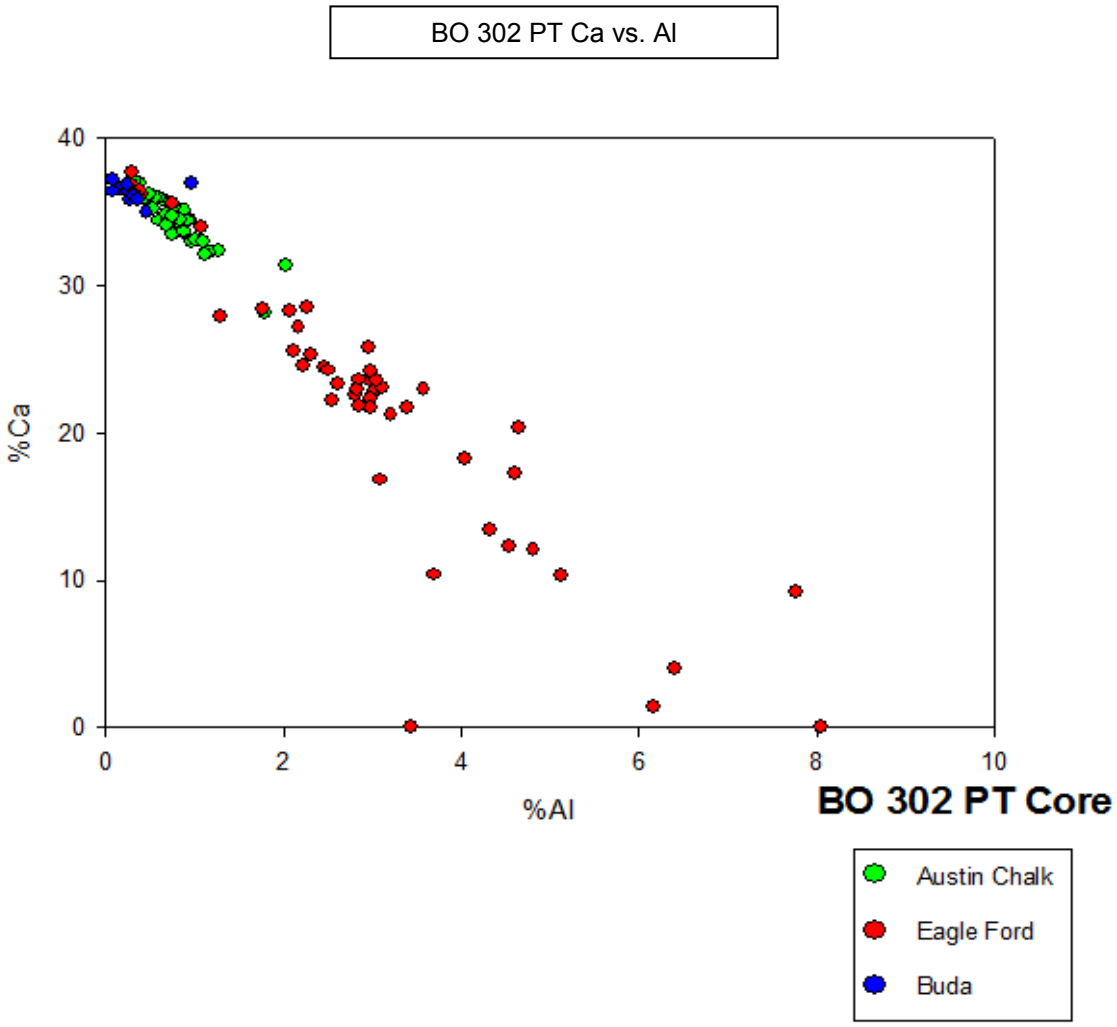

Figure 21. Carbonate richness versus clay in the BO 302 PT core.

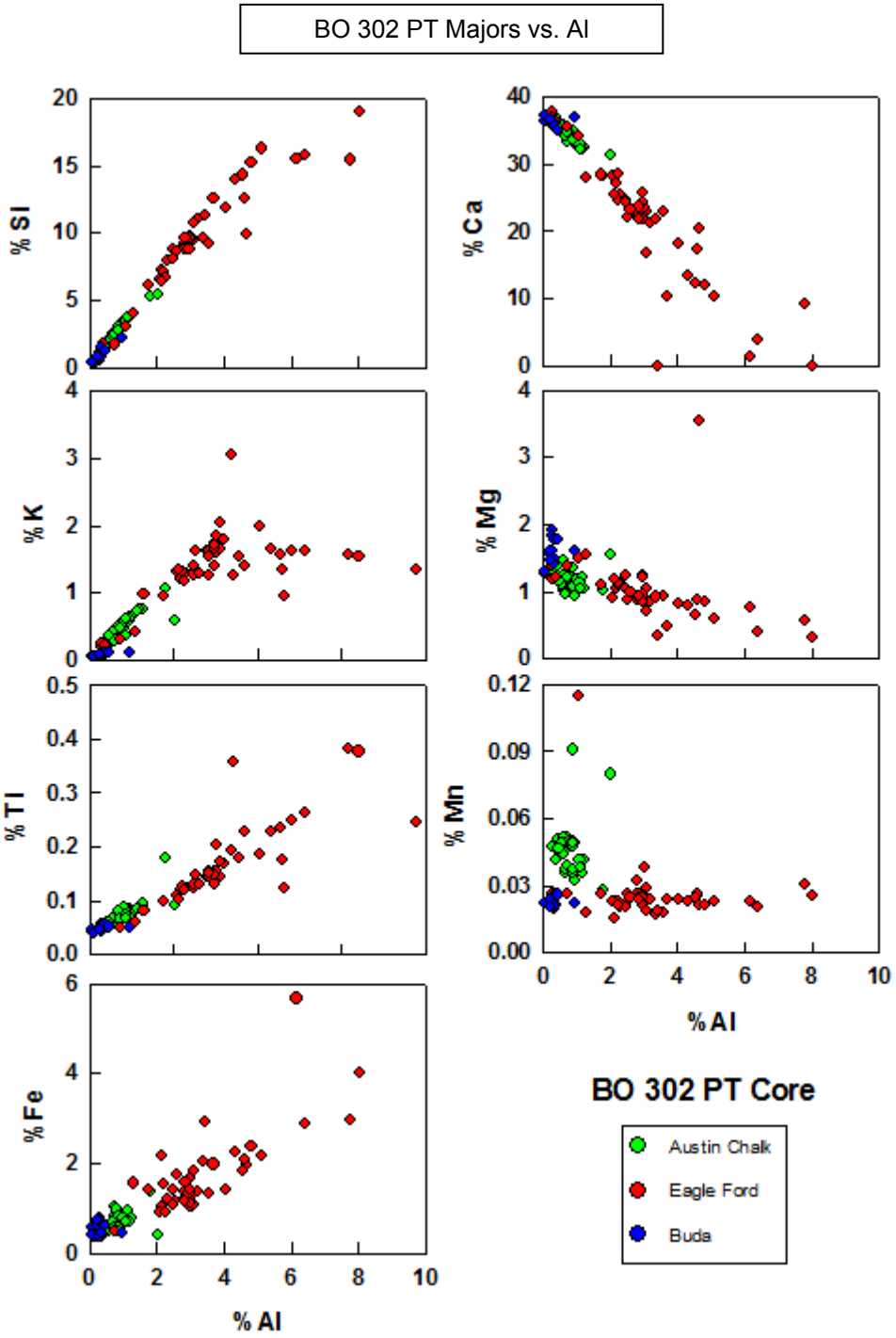

Figure 22. Major elements plotted against Al to qualify clay versus non-clay phase mineral abundances of each element in the BO 302 PT core.

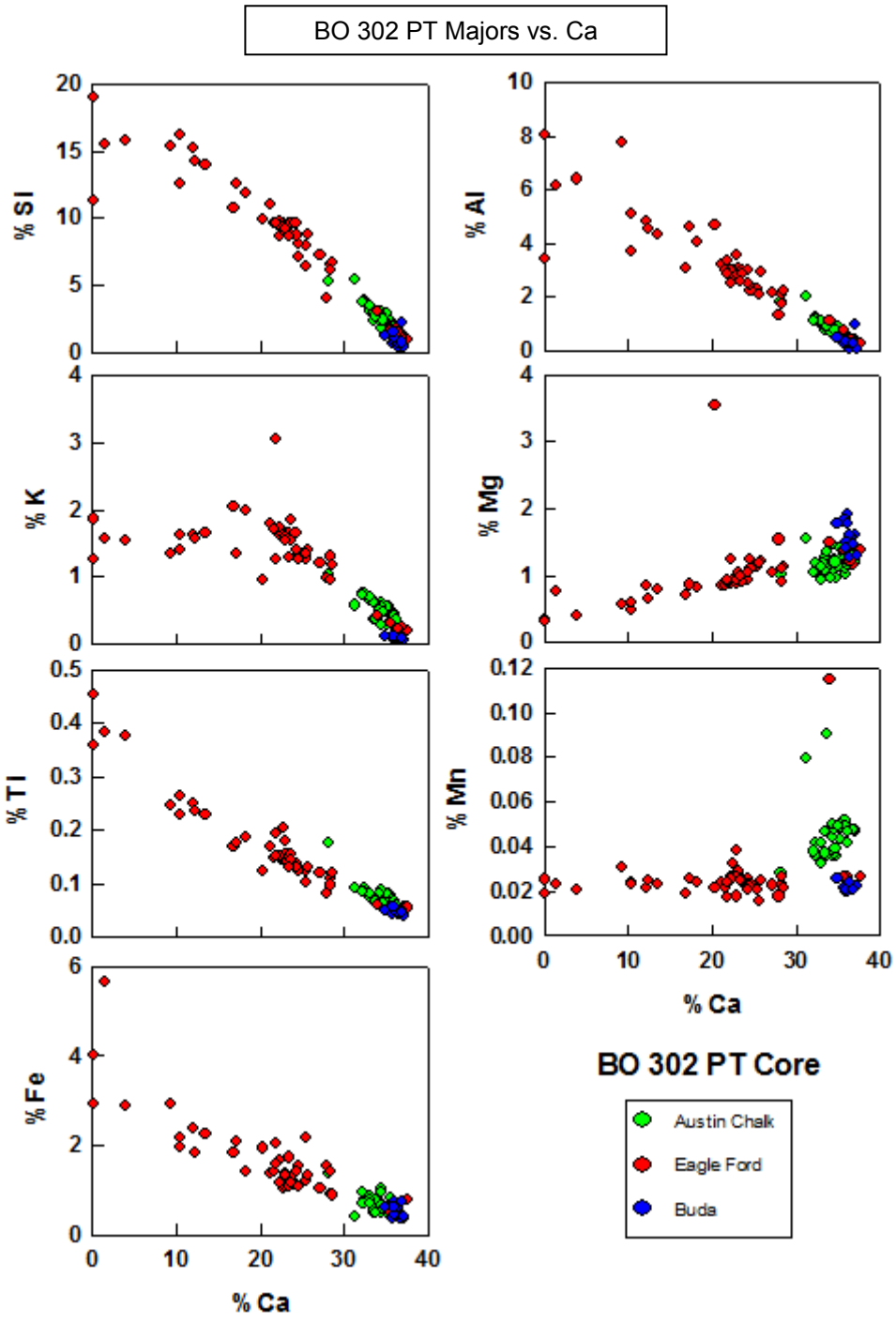

Figure 23. Major elements plotted against Ca to qualify carbonate mineral abundances of each element in the BO 302 PT core.

3.2.5 Calvert Core

Lithologies of the Austin Chalk cluster in the carbonate corner of the ternary diagram, indicating very little sourcing other than carbonates. The Ca/Al plot illustrates a very linear relationship between the two elements, with most plotted points falling in the high Ca, low Al section. This has been interpreted as occasional clay deposition in a predominantly carbonate setting for the Austin Chalk. Mn/Al values for the Austin indicate Mn enrichment associated with low Al values. Mn/Ca values indicate Mn enrichment associated with higher levels of Ca. This has been interpreted as oxic conditions dominating during Austin Chalk and Buda deposition.

The Eagle Ford lithologies follow a very linear line from the carbonate corner of the ternary diagram to the average gray shale point, as defined by Wedepohl (1971). This was interpreted as dominantly carbonate-rich shale which occasionally grades to the level of the average gray shale. This interpretation was strengthened by the Ca/Al plot, showing the Eagle Ford following a linear relationship between the two elements. The Mn/Al plot shows a marked decrease in Mn as Al levels rose. Most Eagle Ford points plotted fell into higher Al values where Mn was greatly reduced. This has been interpreted as anoxic conditions prevailing during much of the deposition of the Eagle Ford.

Several small streaks of increased Ca were throughout the Eagle Ford. Associated with these Ca-rich streaks were increased Mn values. These streaks have been interpreted as minor periods during Eagle Ford deposition where conditions became oxic, allowing Mn to remain fixed as oxy/hydroxides in the sediment.

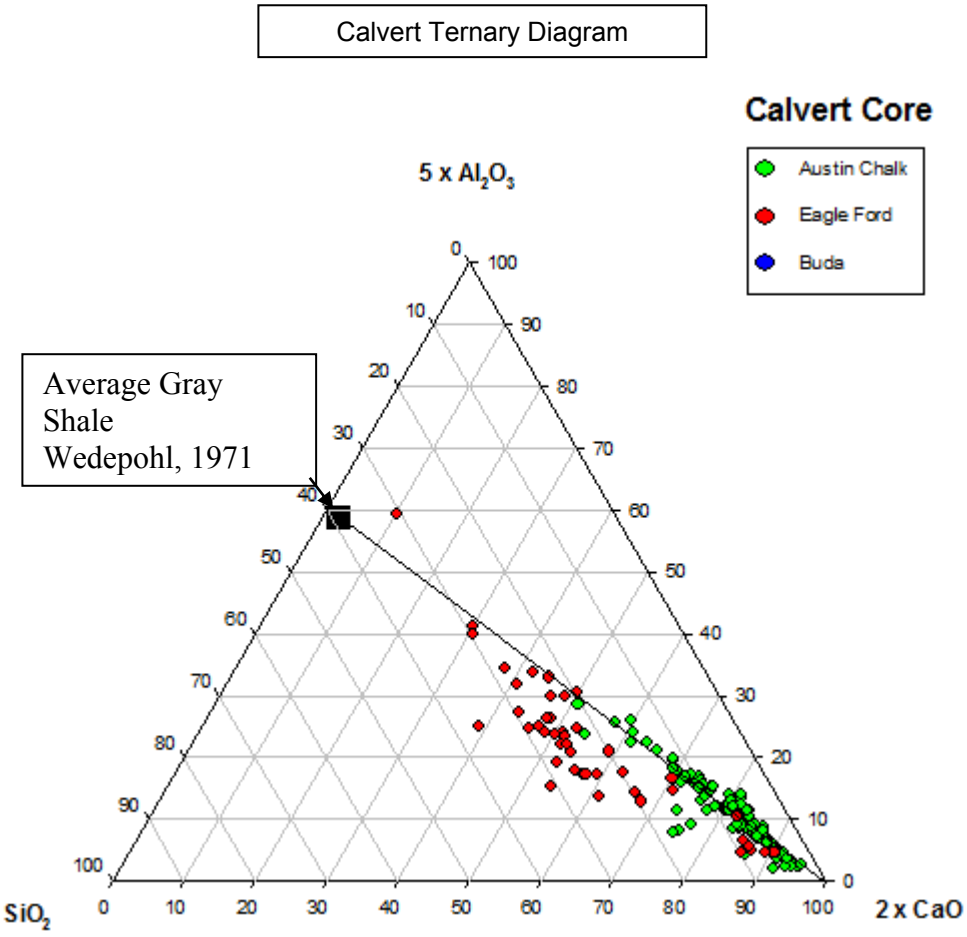

Figure 24. Ternary diagram representing the lithologies of the Austin Chalk and Eagle Ford in the Calvert core, Frio County, Texas.

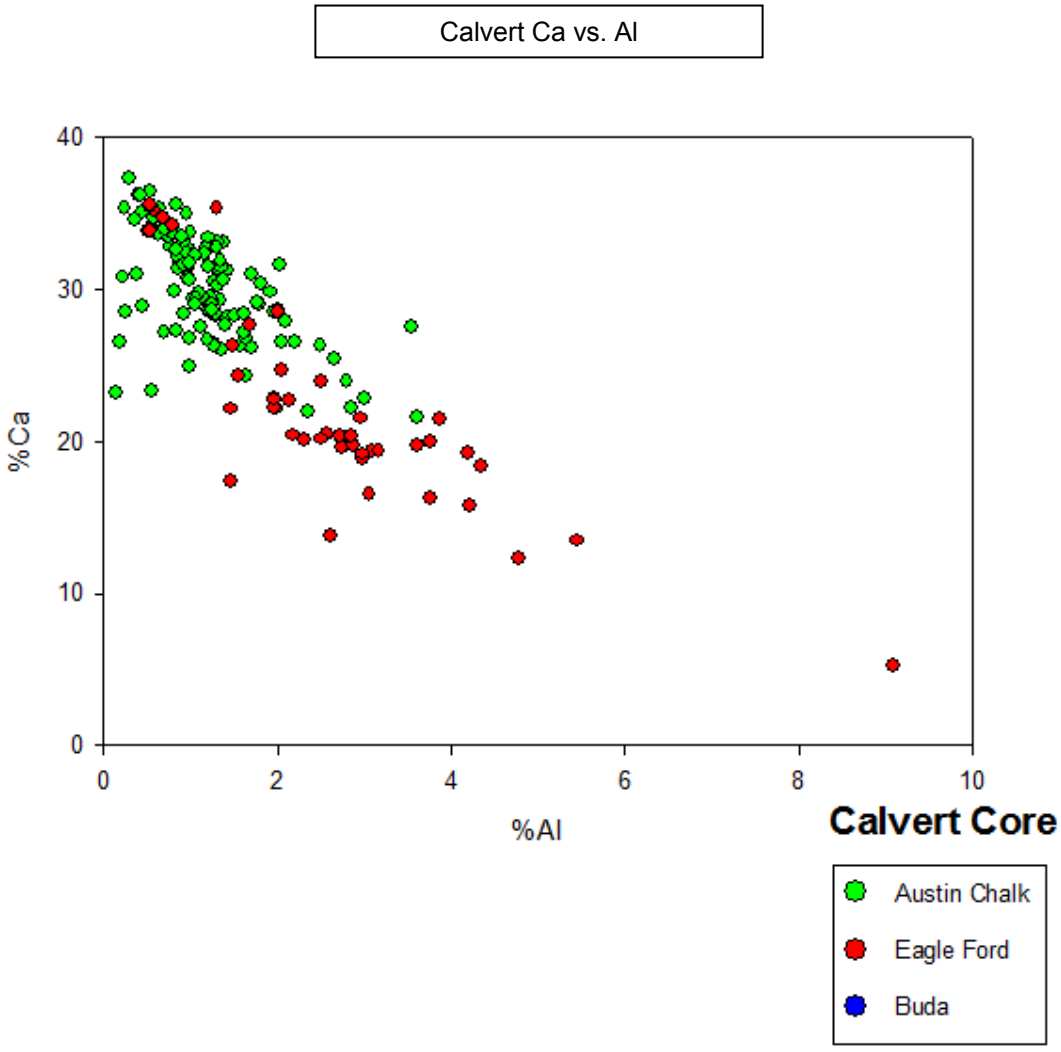

Figure 25. Carbonate richness versus clay in the Calvert core.

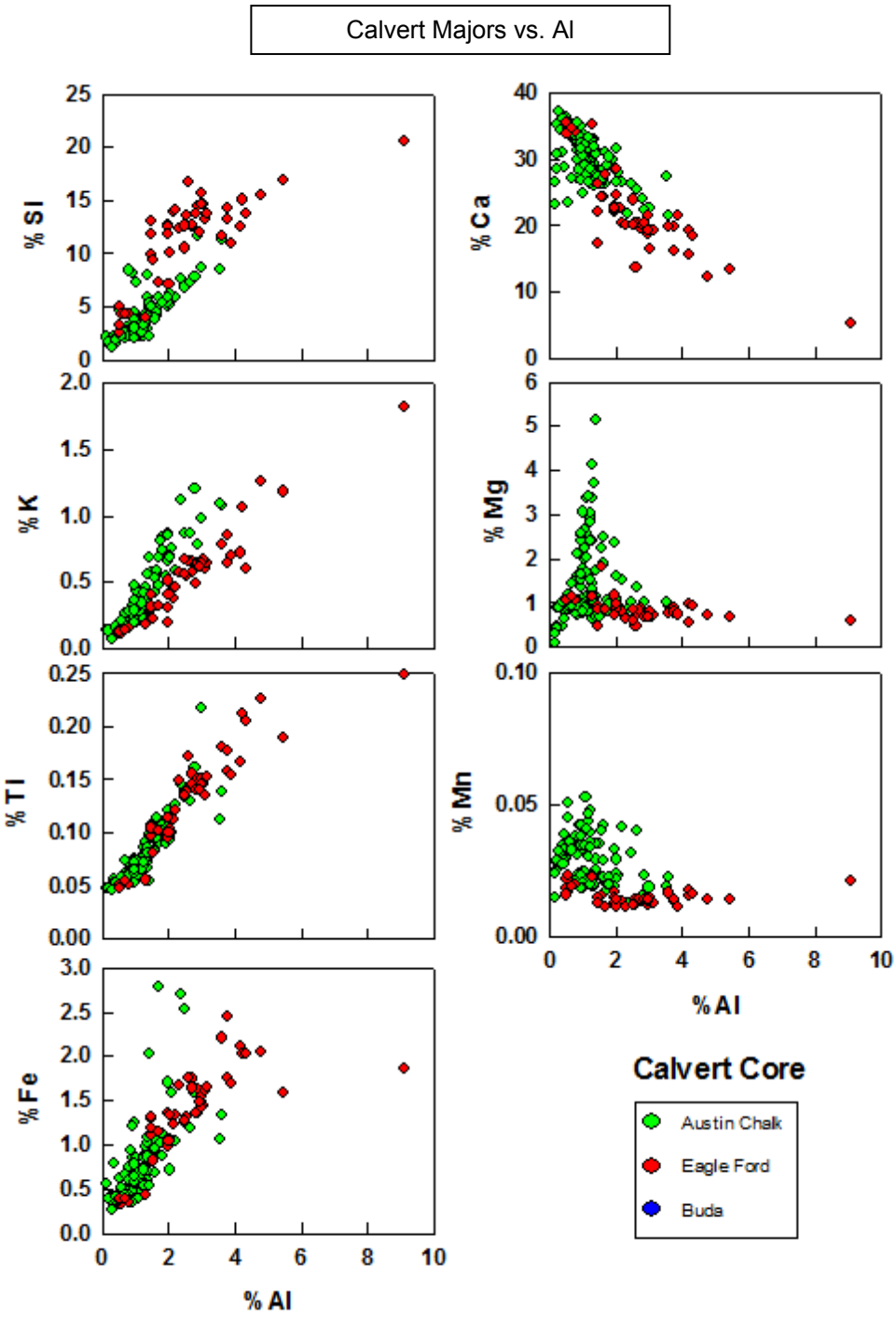

Figure 26. Major elements plotted against Al to qualify clay versus non-clay phase mineral abundances of each element in the Calvert core.

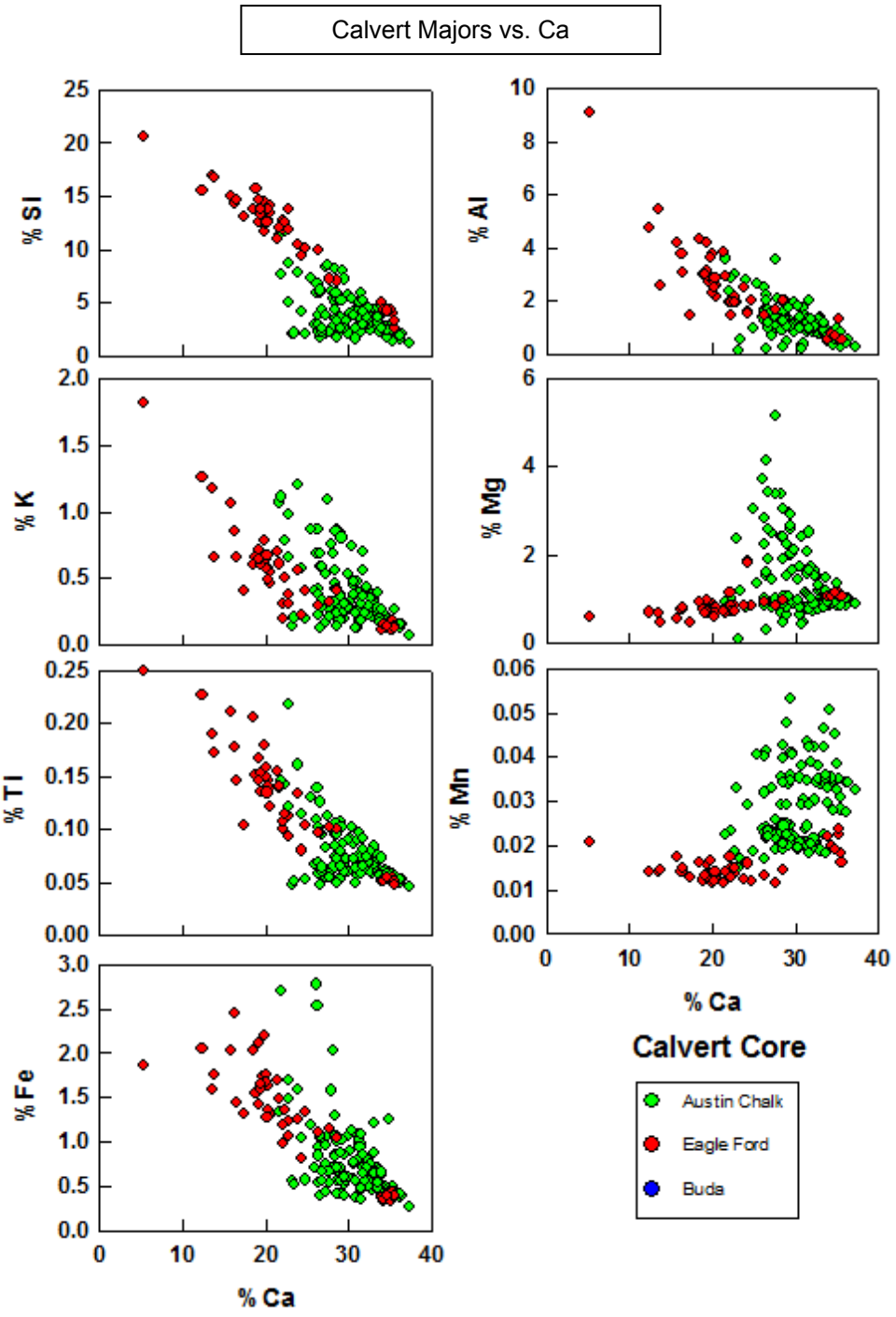

Figure 27. Major elements plotted against Ca to qualify carbonate mineral abundances of each element in the Calvert core.

3.3 Trace Element Analysis

Figures 28-33 represent major and trace element concentrations plotted against depth where a direct visual comparison of the concentrations may be made. This format is similar to the format used in conventional electrical well logs. This is also the simplest format to perform correlation between two different cores, or among a group of cores. Each core has been designed to show all of the collected data depths, with an extra plot added from the Calvert core which isolates the Eagle Ford. The Eagle Ford was isolated in the Calvert in order to provide a more detailed look at the section of interest. The Mn/Al scale was altered from the first Calvert plot because the Mn/Al values from the Austin Chalk effectively suppressed any details present in the Eagle Ford Mn/Al values.

Using U, V, and Mo concentrations as oxic level indicators (Shaw, Geiskes, Jahnke, 1990; Algeo and Maynard, 2004; Smith, 2010; Jenkyns, 2010), an interpretation may be made of bottom water conditions, and correlations may be made between two cores or among several cores. When U and V enrichment is present without a correlative enrichment in Mo, it has been interpreted as suboxic/anoxic, but not euxinic (lacking free H_2S). When concurrent enrichment in U, V, and Mo were observed, this was indicative of euxinic conditions (Tribovillard et al., 2006; Soua, 2010)

3.3.1 ACC 1 Core

U, V, and Mo concentrations in the Austin Chalk and Buda were almost completely absent (**Figure 28**). The Eagle Ford, especially when viewing U concentrations, stood out from the Austin Chalk and Buda. U values were greatly increased in the Ca and Mn free zone from the top Buda up to the oxic/suboxic cyclic zone, above which the levels increase again up to the base of the Austin Chalk.

V values within the Eagle Ford appeared to be highest in the oxic/suboxic cyclical zone, but showed increased values throughout the entire Eagle Ford section. V concentrations,

although independently variable, did correlate well with U values, showing increased values where U was enriched, and decreased values where U was not enriched.

Mo concentrations showed some different values when compared back to U and V within the Eagle Ford. Although some increased values were noted in the Ca and Mn free zone just above the Buda, the highest concentrations fell into the oxic/suboxic cyclical zone. These increases correlated better with V concentration increases than with U. The Ca and Mn free zone below the Austin Chalk displayed a section with very low Mo concentrations.

When combing these three trace element concentrations and comparing them directly to each other, the following interpretation was made. The Ca and Mn free zone from the top of the Buda to the cyclical zone was deposited under suboxic conditions, but free H_2S was not present in the bottom waters for the majority of the deposition. The cyclical zone above that went back and forth between periods of oxic bottom waters, indicated by increased Mn and decreased U, V, and Mo concentrations, and periods when the bottom waters were likely euxinic in nature, indicated by increased concentrations of U, V, and Mo as well as depletion of Mn. The Ca and Mn free zone above the cyclical zone up to the Austin Chalk was deposited under suboxic bottom water conditions, but did not have free H_2S in the water column, as indicated by U and V enrichment without corresponding Mo enrichment.

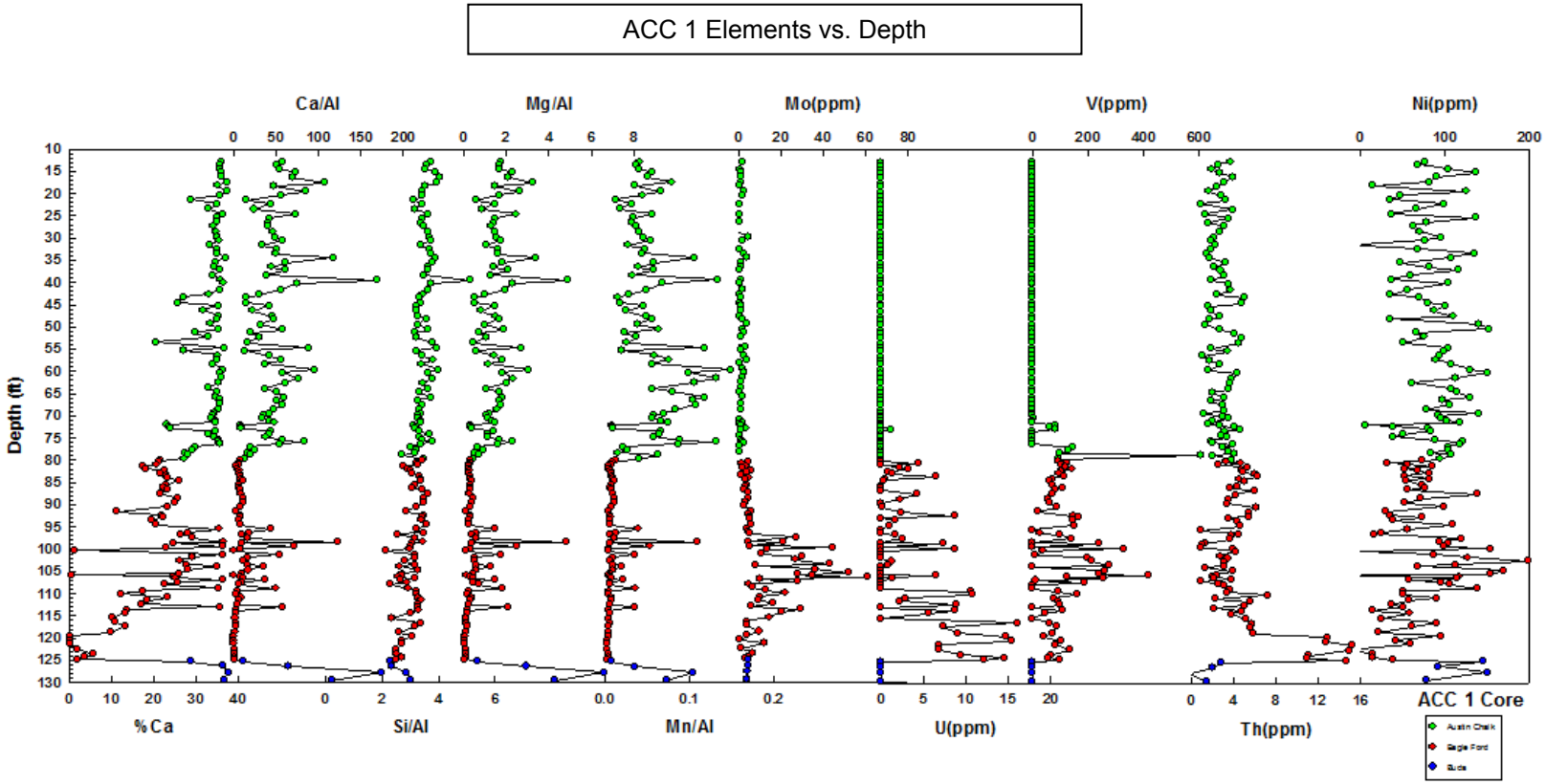

Figure 28. Major and trace elemental concentrations plotted against depth in the ACC 1 core.

3.3.2 BT 221 Core

As with the ACC 1 core, U, V, and Mo concentrations in the Austin Chalk and Buda were almost completely absent (**Figure 29**). The Eagle Ford, especially when viewing U concentrations, stood out from the Austin Chalk and Buda. U values were greatly increased in the Ca and Mn free zone from the top Buda up to the oxic/suboxic cyclic zone, above which the levels increase again up to the base of the Austin Chalk.

V values within the Eagle Ford appeared to be highest in the oxic/suboxic cyclical zone, but showed increased values throughout the entire Eagle Ford section. V concentrations, although independently variable, did correlate well with U values, showing increased values where U was enriched, and decreased values where U was not enriched.

Mo concentrations showed some different values when compared back to U and V within the Eagle Ford. Although some increased values were noted in the Ca and Mn free zone just above the Buda, the highest concentrations fell into the oxic/suboxic cyclical zone. These increases correlated better with V concentration increases than with U. The Ca and Mn free zone below the Austin Chalk displayed a section with very low Mo concentrations.

When combing these three trace element concentrations and comparing them directly to each other, the following interpretation was made. The Ca and Mn free zone from the top of the Buda to the cyclical zone was deposited under suboxic conditions, but free H_2S was not present in the bottom waters for the majority of the deposition. The cyclical zone above that went back and forth between periods of oxic bottom waters, indicated by increased Mn and decreased U, V, and Mo concentrations, and periods when the bottom waters were likely euxinic in nature, indicated by increased concentrations of U, V, and Mo as well as depletion of Mn. The Ca and Mn free zone above the cyclical zone up to the Austin Chalk was deposited under suboxic bottom water conditions, but did not have free H_2S in the water column for the majority of the zone, as indicated by U and V enrichment without corresponding Mo enrichment. One

noticeable increase of Mo was represented at 59.5 feet, which indicated a very short period of euxinia, but quickly returned to anoxic conditions without the presence of H_2S.

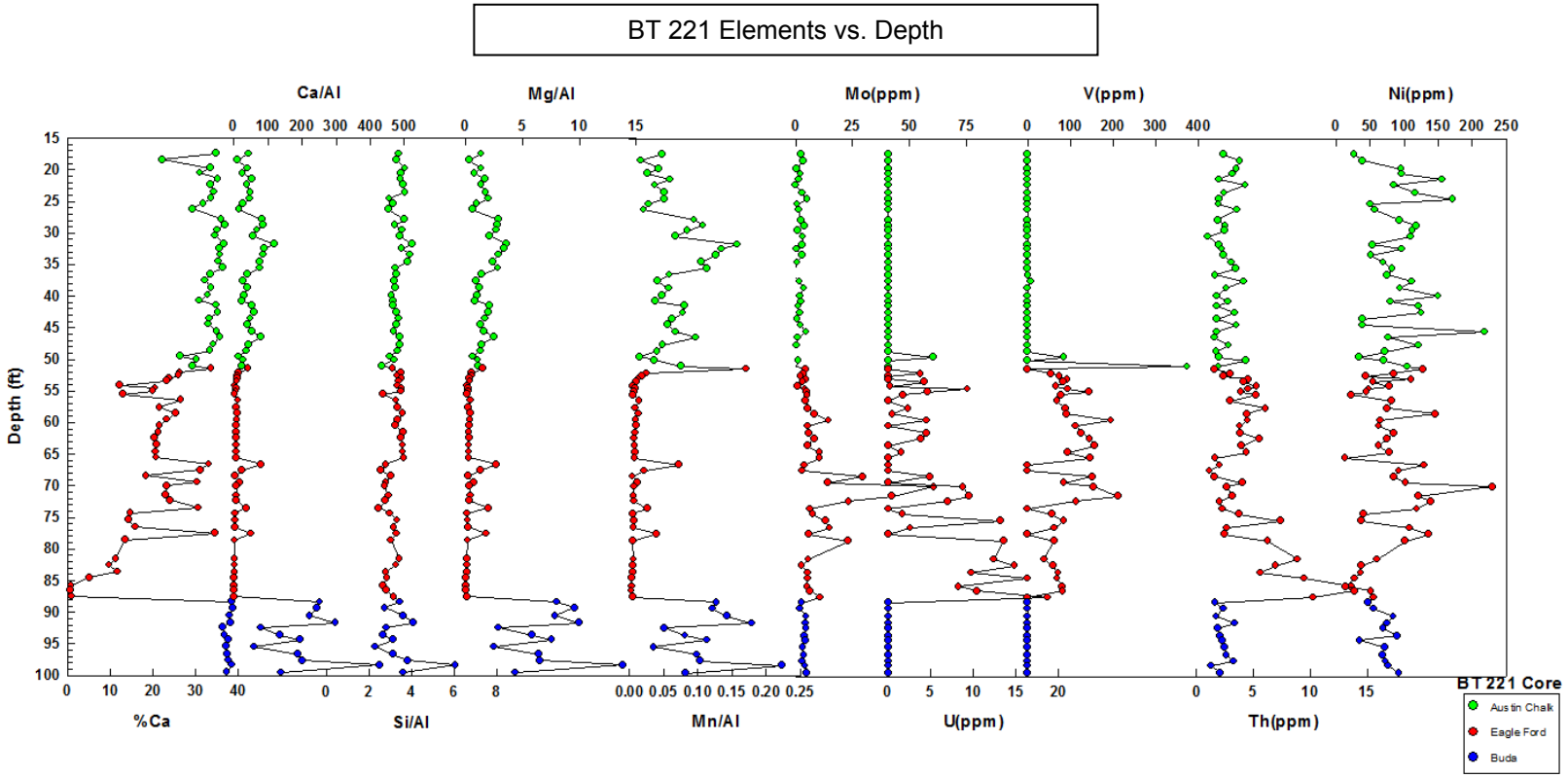

Figure 29. Major and trace elemental concentrations plotted against depth in the BT 221 core.

3.3.3 BT-222 Core

As with the previous cores, U, V, and Mo concentrations in the Austin Chalk and Buda were almost completely absent (**Figure 30**). The Eagle Ford, especially when viewing U concentrations, stood out from the Austin Chalk and Buda. U values were greatly increased in the Ca and Mn free zone from the top Buda up to the oxic/suboxic cyclic zone, above which the levels increase again up to the base of the Austin Chalk.

V values within the Eagle Ford appeared to be highest in the oxic/suboxic cyclical zone, but showed increased values throughout the entire Eagle Ford section. V concentrations, although independently variable, did correlate well with U values, showing increased values where U was enriched, and decreased values where U was not enriched.

Mo concentrations showed some different values when compared back to U and V within the Eagle Ford. Although some increased values were noted in the Ca and Mn free zone just above the Buda, the highest concentrations fell into the oxic/suboxic cyclical zone. These increases correlated better with V concentration increases than with U. The Ca and Mn free zone below the Austin Chalk displayed a section with very low Mo concentrations.

When combing these three trace element concentrations and comparing them directly to each other, the following interpretation was made. The Ca and Mn free zone from the top of the Buda to the cyclical zone was deposited under suboxic conditions, but free H_2S was not present in the bottom waters for the majority of the deposition. The cyclical zone above that went back and forth between periods of oxic bottom waters, indicated by increased Mn and decreased U, V, and Mo concentrations, and periods when the bottom waters were likely euxinic in nature, indicated by increased concentrations of U, V, and Mo as well as depletion of Mn. The Ca and Mn free zone above the cyclical zone up to the Austin Chalk was deposited under suboxic bottom water conditions, but did not have free H_2S in the water column for the majority of the zone, as indicated by U and V enrichment without corresponding Mo enrichment.

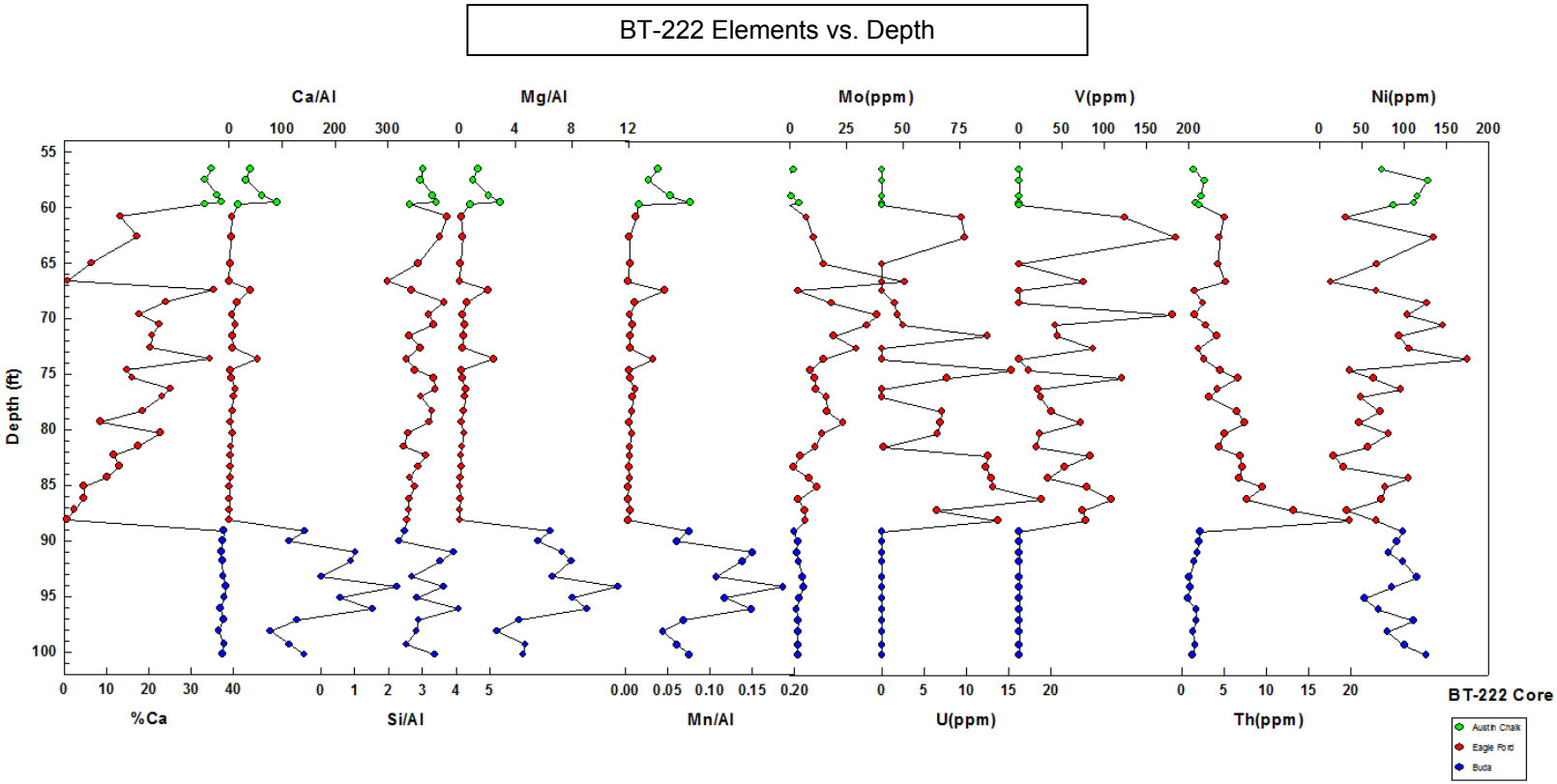

Figure 30. Major and trace elemental concentrations plotted against depth in the BT-222 core.

3.3.4 BO 302 PT Core

As with the previous cores, U, V, and Mo concentrations in the Austin Chalk and Buda were almost completely absent (**Figure 31**). The Eagle Ford, especially when viewing U concentrations, stood out from the Austin Chalk and Buda. U concentrations largely fell outside detectable levels, and values below zero were represented as zero. U values were greatly increased in the Ca and Mn free zone from the top Buda up to the oxic/suboxic cyclic zone, above which the levels increase again up to the base of the Austin Chalk.

V values within the Eagle Ford appeared to be highest in the oxic/suboxic cyclical zone, but showed increased values throughout the entire Eagle Ford section. V concentrations, although independently variable, did correlate well with U values, showing increased values where U was enriched, and decreased values where U was not enriched. The largest cluster of high V concentrations was seen in the zone between the oxic/suboxic cyclical zone and the Austin Chalk.

Mo concentrations showed some different values when compared back to U and V within the Eagle Ford. Although some increased values were noted in the Ca and Mn free zone just above the Buda, the highest concentrations fell into the oxic/suboxic cyclical zone. These increases correlated better with V concentration increases than with U. The Ca and Mn free zone below the Austin Chalk displayed a section with very low Mo concentrations.

When combing these three trace element concentrations and comparing them directly to each other, the following interpretation was made. The Ca and Mn free zone from the top of the Buda to the cyclical zone was deposited under suboxic conditions, but free H_2S was not present in the bottom waters for the majority of the deposition. The cyclical zone above that went back and forth between periods of oxic bottom waters, indicated by increased Mn and decreased U, V, and Mo concentrations, and periods when the bottom waters were likely euxinic in nature, indicated by increased concentrations of U, V, and Mo as well as depletion of Mn. The Ca and Mn free zone above the cyclical zone up to the Austin Chalk was deposited under suboxic

bottom water conditions, having periodic free H_2S in the water column for the majority of the zone, as indicated by U, V, and Mo enrichments. This observation differs from the previous three cores from Central Texas, which may point to either poor data or a slightly different depositional sub-setting.

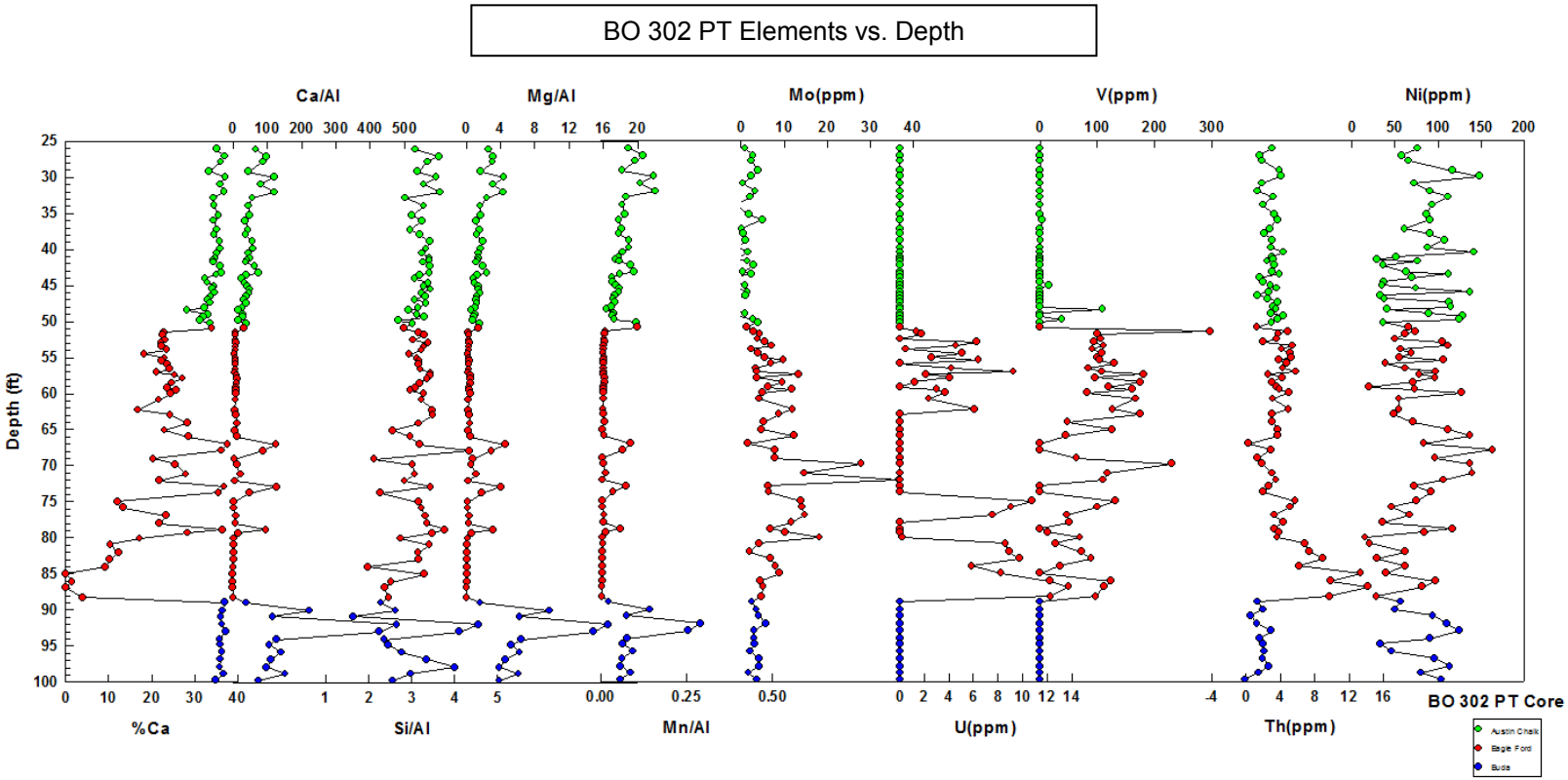

Figure 31. Major and trace elemental concentrations plotted against depth in the BO 302 PT core.

3.3.5 Calvert Core

U, V, and Mo concentrations in the Austin Chalk were almost completely absent. The Eagle Ford, especially when viewing Mo and V concentrations, stood out from the Austin Chalk.

V values within the Eagle Ford showed enrichment higher than was found in the Austin Chalk. V concentrations, although independently variable, did correlate well with U values, showing increased values where U was enriched, and decreased values where U was not enriched.

Mo concentrations showed similar values when compared back to U and V within the Eagle Ford. Mo enrichment was easily correlated to U and V enrichments. These increases correlated well with both U and V concentration increases.

When combing these three trace element concentrations and comparing them directly to each other, the following interpretation was made. Small zones of Ca and Mn enrichment were noted through the Eagle Ford, all of which corresponded directly to drops in U, V, and Mo concentrations, indicating small periods of oxic bottom water deposition. The majority of the Eagle Ford represented by the core indicated decreased Mn and increased U, V, and Mo concentrations, indicating euxinic conditions dominated Eagle Ford deposition.

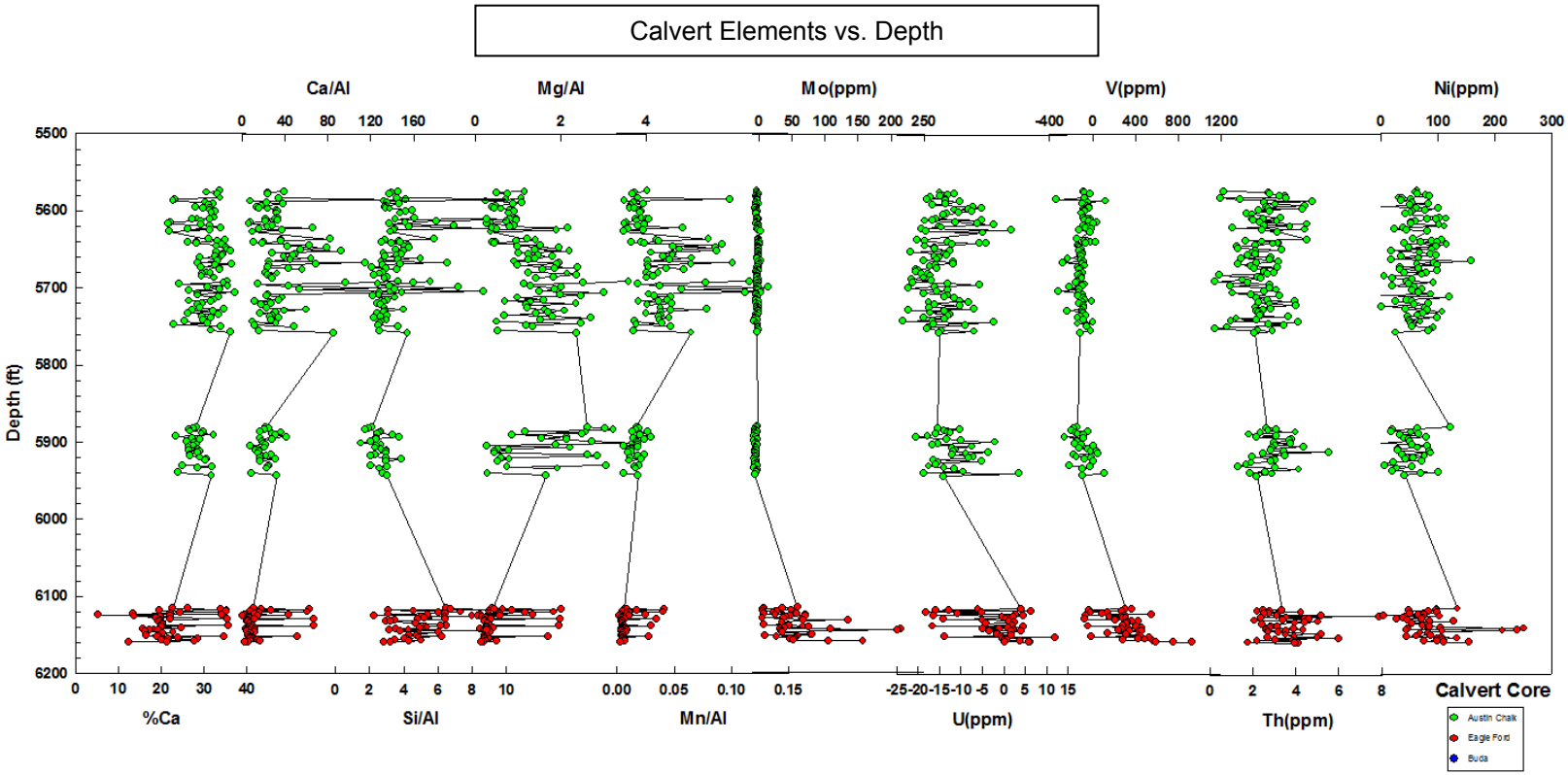

Figure 32. Major and trace elemental concentrations plotted against depth in the Calvert core.

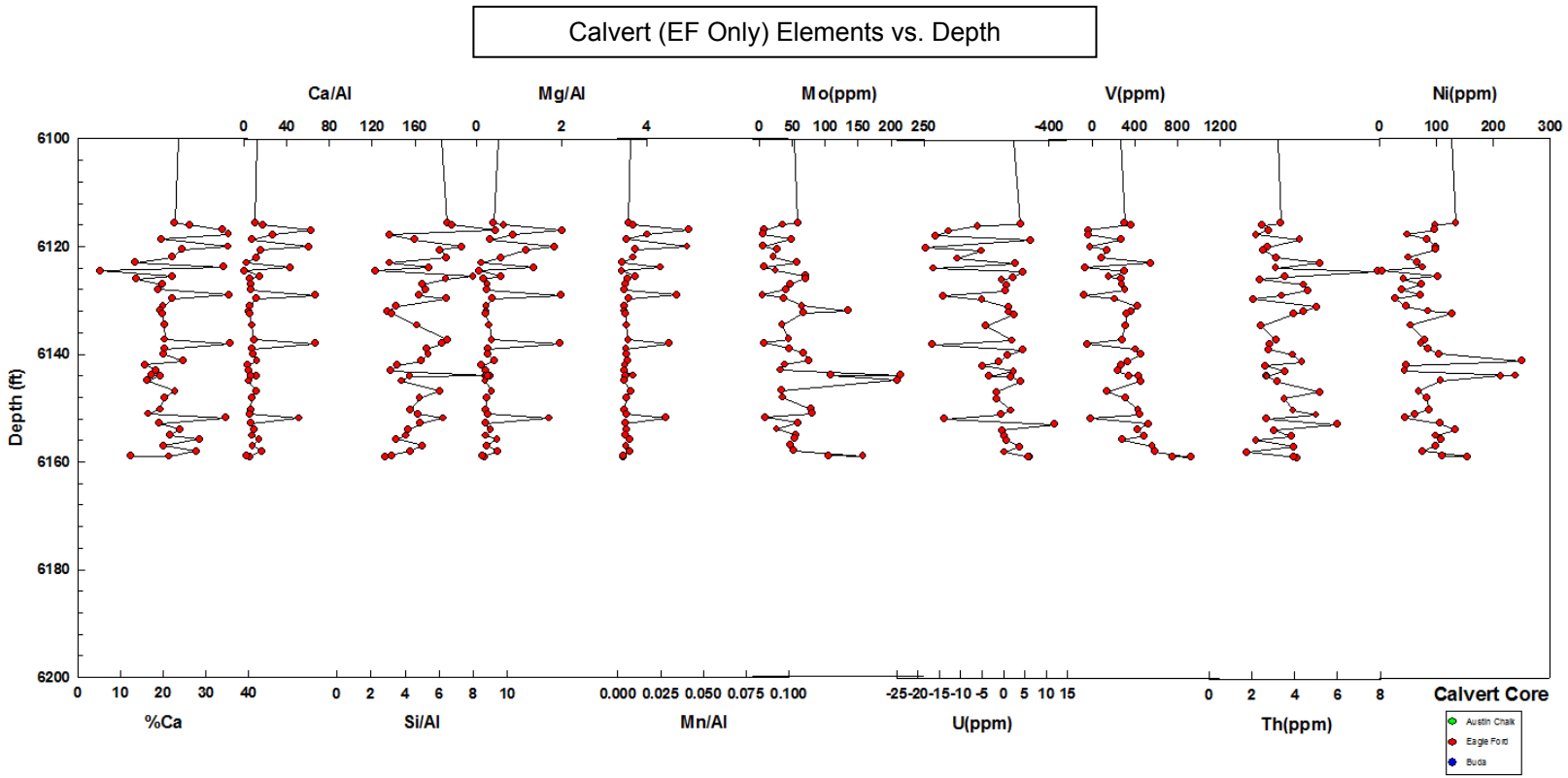

Figure 33. Major and trace elemental concentrations plotted against depth in the Calvert core. The Eagle Ford section has been isolated for clarity. Note: the scale for Mn/Al was changed to provide better resolution of subtle changes and to make correlation easier.

CHAPTER 4

DISCUSSION

The following discussion focuses on the Cenomanian-Turonian Eagle Ford. The Austin Chalk and Buda are also discussed as contrasting frames of reference against the Eagle Ford. In the cores utilized in this study from Central Texas, the Austin Chalk and Buda lithologically and geochemically provide distinct boundaries for the delineation of the Eagle Ford.

4.1 Depositional Environment

Figures 34-37 illustrate the geochemically unique nature of the Eagle Ford when compared to the Austin Chalk and Buda. The Austin Chalk and Buda display elevated concentrations of Mn, indicating likely oxic depositional conditions, while having low concentrations of trace elements, associated with anoxic environments. According to the geochemical makeup of each, the Austin Chalk and Buda were deposited under oxic conditions. The Eagle Ford, in general, displayed elevated concentrations of trace elements associated with anoxic conditions and low concentrations of Mn. According to the geochemical makeup of the Eagle Ford, anoxic conditions dominated during much of the deposition.

4.2 Correlation

4.2.1 Major Element Correlation

As the Calvert core had an incomplete Eagle Ford section and was missing the Eagle Ford/Austin Chalk (EF/AC) and Eagle Ford/Buda (EF/Buda) contacts, the Calvert was excluded from the following correlation. Using only major elements for correlation was not the preferred method, but using Ca and Mn concentrations was somewhat useful in determining major contacts such as the aforementioned EF/AC and EF/Buda. The Eagle Ford, in general, contains low levels of both Ca and Mn when compared to the underlying Buda and overlying Austin Chalk. The first noticeable increase in Ca and Mn concentrations within the Eagle Ford was noticed approximately ten feet above the EF/Buda contact. The same Ca and Mn increase was observed in all four cores from Central Texas. This change seemed to be the beginning of a small series of oxic/anoxic cycles, covering up to 20 feet in the ACC 1 core, which appeared to have the most complete section of Eagle Ford. The interval of oxic/anoxic cyclicity varies in

thickness and number of occurrences in each core, but the section as a whole was present in all and was correlatable. No attempt was made to correlate individual cycles. A quiet period of presumed anoxic conditions followed up until the EF/AC contact. The quiet interval was approximately 15 feet thick in all cores except the BT-222, where it was about seven feet thick. The EF/AC contact defined by the overall increase of Ca and Mn in the BT-222 core was very abrupt, whereas it was slightly more gradual in the other cores, indicating a possible truncation of the Eagle Ford section in the BT-222. The Austin Chalk and Buda are readily identifiable using Ca and Mn concentrations. The Austin Chalk and Buda appeared to have been deposited in more oxic waters, as the Mn concentrations in both were much higher than those of the Eagle Ford.

4.2.2 Trace Element Correlation Summary

Figures 34-37 graphically represent the interpreted correlations discussed in this study. Independently, the use of major element concentrations may be used to create a good lithological model, useful for correlating changes in lithology and formation interfaces, while trace element concentrations may be used to build a redox model, useful for correlating redox events and changes from well to well. Although each method yields a useful correlation model, using either method independent of the other does not yield the entire picture, which limits the effectiveness of the correlations performed. In order to build the most effective correlation model possible based on XRF, both the major element concentrations and the trace metal concentrations must be included in the analytical process. The previously described interpretations made use of both sets of data to not only describe the lithology, but also identify redox conditions associated with said lithologies. Major element data from the cores in Central Texas identified a zone of cyclical shale/carbonate deposition and spoke to the qualitative nature of the redox conditions while the trace metal data quantified the redox conditions, adding another level of detail and correlatability.

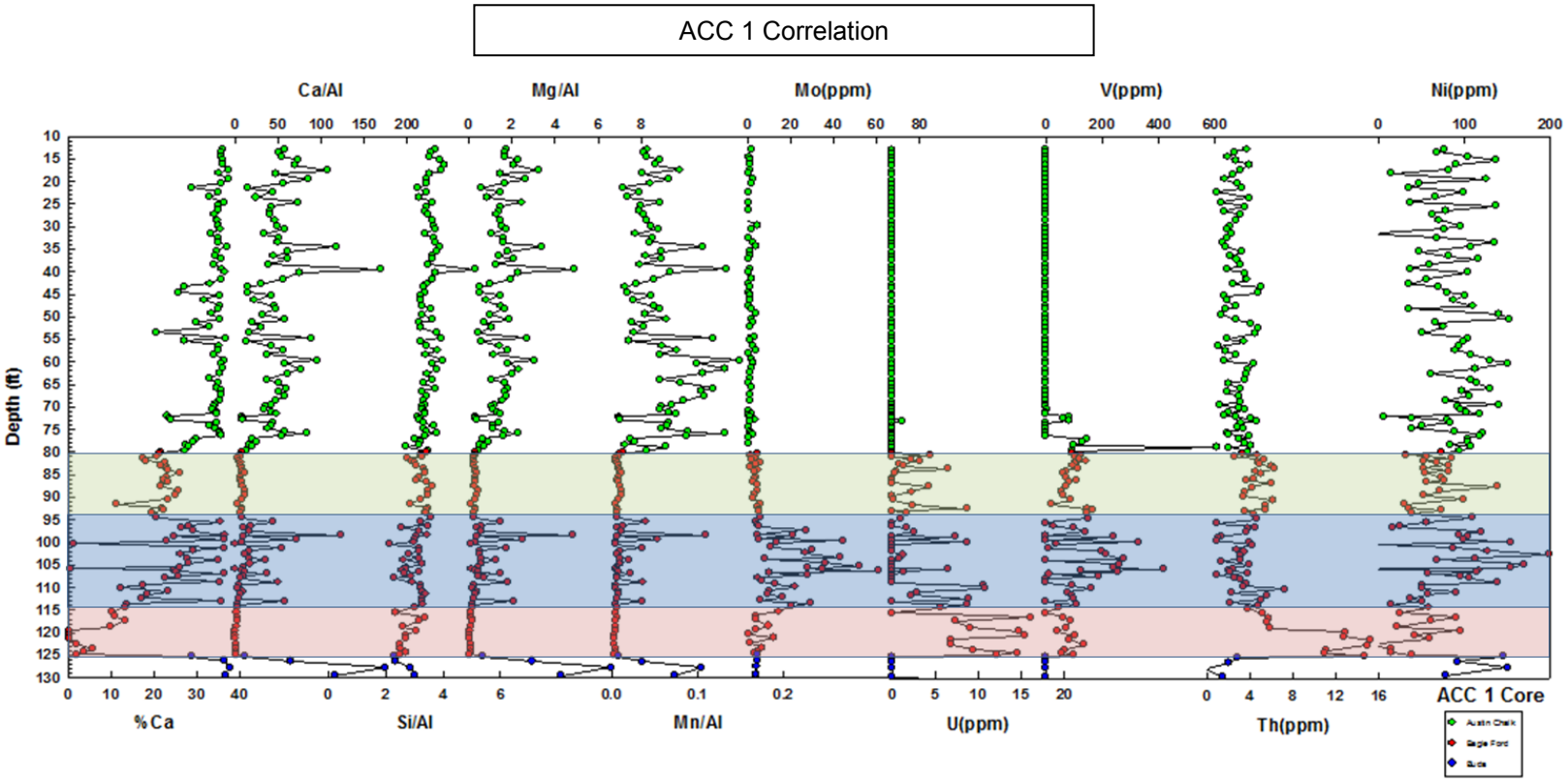

Figure 34. Correlation of the three chemostratigraphically distinct sections of the Eagle Ford from the ACC 1 core. Light green fill represents the quiet section from the Austin Chalk to the cyclic section of the Eagle Ford. The blue color fill represents the cyclical section of the Eagle Ford with greater amounts of Ca. The red color fill represents the section of high U content from the top Buda to the base of the cyclical section.

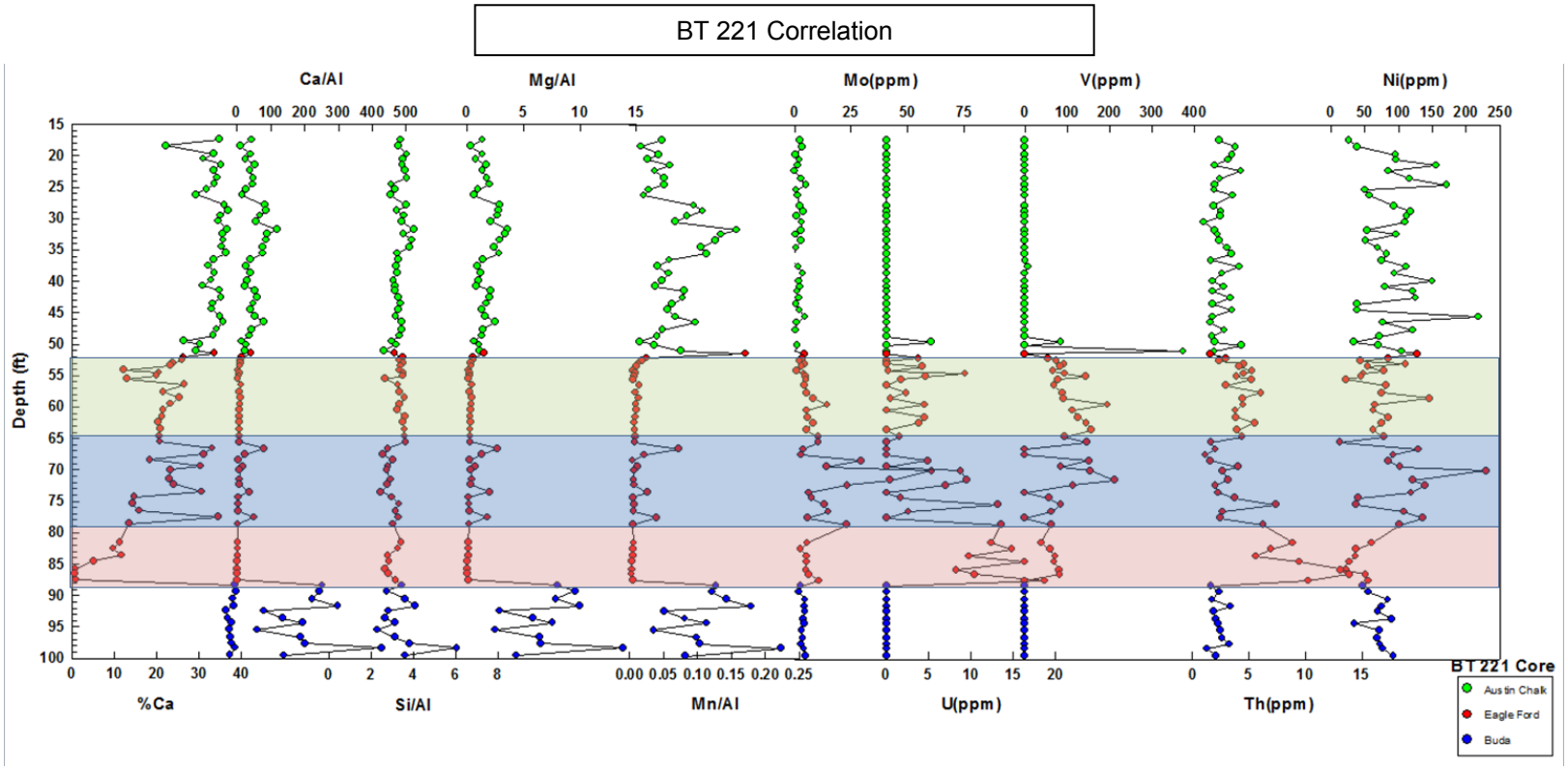

Figure 35. Correlation of the three chemostratigraphically distinct sections of the Eagle Ford from the BT 221 core. Light green fill represents the quiet section from the Austin Chalk to the cyclic section of the Eagle Ford. The blue color fill represents the cyclical section of the Eagle Ford with greater amounts of Ca. The red color fill represents the section of high U content from the top Buda to the base of the cyclical section.

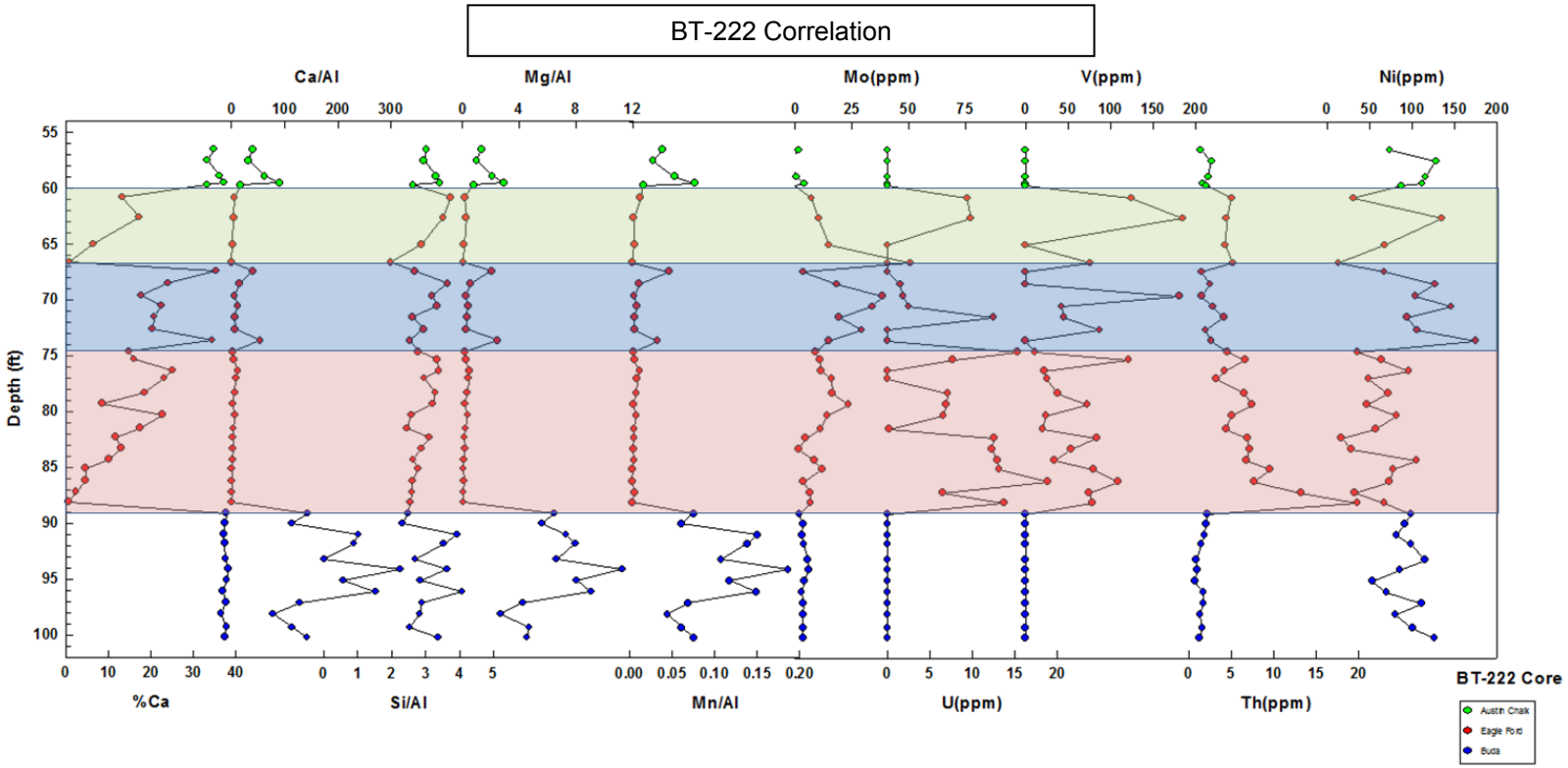

Figure 36. Correlation of the three chemostratigraphically distinct sections of the Eagle Ford from the BT-222 core. Light green fill represents the quiet section from the Austin Chalk to the cyclic section of the Eagle Ford. The blue color fill represents the cyclical section of the Eagle Ford with greater amounts of Ca. The red color fill represents the section of high U content from the top Buda to the base of the cyclical section.

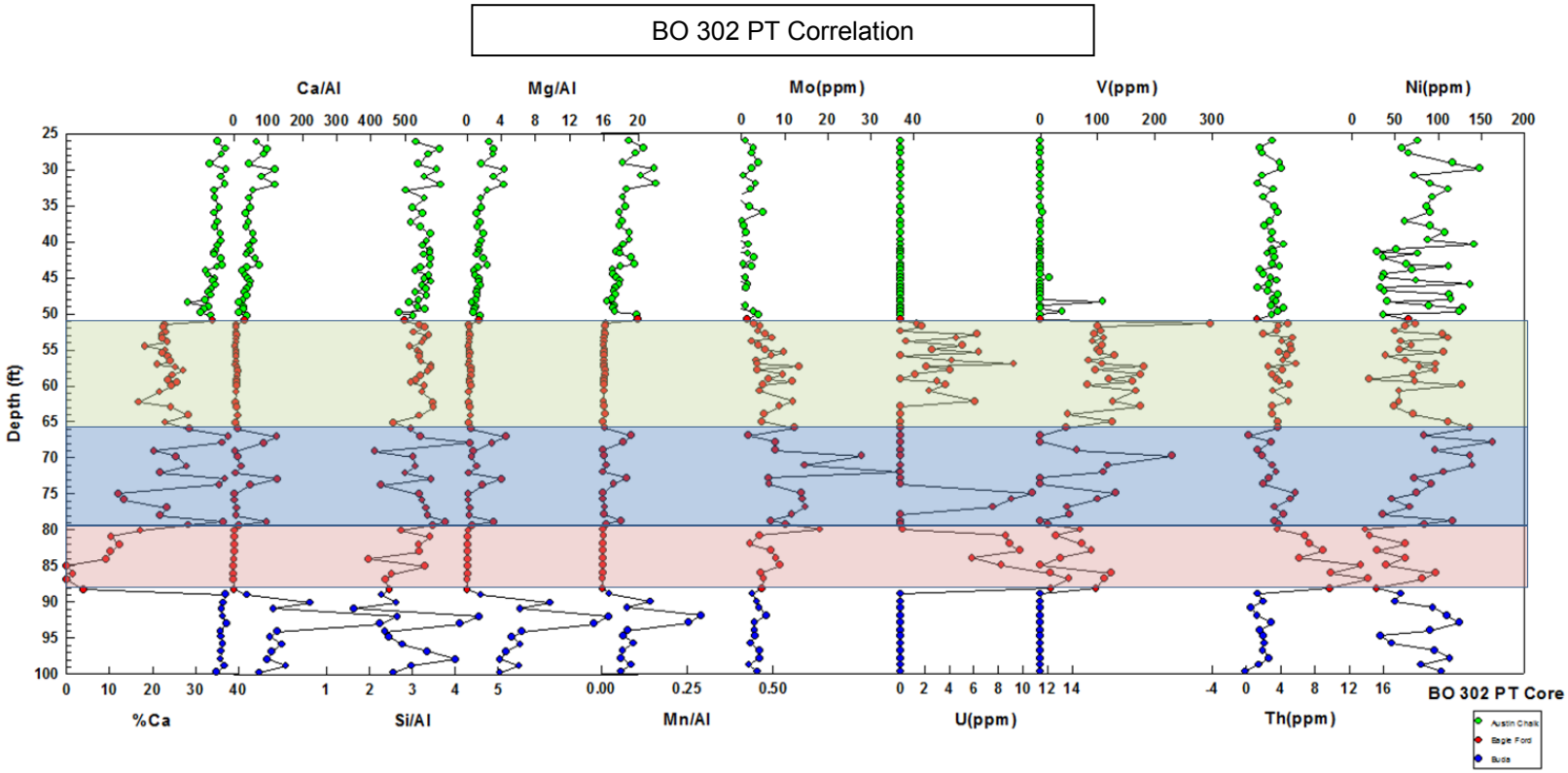

Figure 37. Correlation of the three chemostratigraphically distinct sections of the Eagle Ford from the BO 302 PT core. Light green fill represents the quiet section from the Austin Chalk to the cyclic section of the Eagle Ford. The blue color fill represents the cyclical section of the Eagle Ford with greater amounts of Ca. The red color fill represents the section of high U content from the top Buda to the base of the cyclical section.

CHAPTER 5

CONCLUSIONS

5.1 Conclusions

The application of geochemical data obtained by XRF provides an in-depth picture of the past. Through analysis, it was possible to reconstruct the depositional environment of the rocks of the Upper Cretaceous, allowing the construction of a model for correlation. Previously, correlation was limited to the use of physical rock descriptions and the interpretation of electric logs. Through the development of geochemical methods like XRF, another key tool has been added to the explorationist's toolbox, allowing a more detailed analysis and frame of reference. XRF, as a tool, has been able to overcome some of the limitations of physical rock description and electric logs. This study was done using whole rock cores, which is an expensive task to undertake, and also increases the risks of drilling a well. XRF analysis may be done using cuttings collected as the well is drilling, eliminating some of the extra costs and risks involved with obtaining whole core. Cuttings analysis will not completely replace whole core analysis, as core may be analyzed on a much smaller scale, but it is certainly a cheaper option that should be considered. In this study, the focus was on the Eagle Ford, which has been known as a source rock for decades, but has more recently been drilled and fracture treated a reservoir as well, with positive results. The Eagle Ford in Central Texas is neither a source nor a reservoir as it is too shallow, but is easily obtainable for study. This study has determined the anoxic nature of the depositional environment of the Eagle Ford found in four cores in Central Texas and one partial core in South Texas. Although the particulars of the Eagle Ford are subject to change laterally, the general features described in this study appear to hold true over great distances. The anoxic conditions found in the cores analyzed are echoed in rocks of similar age from Europe, South America, and Africa, lending more credence to the idea of an Ocean Anoxia Event. This idea may be applied to other areas with the same age rocks residing in conditions suitable for hydrocarbon generation. This idea is not only compatible with shales from the

Cenomanian-Turonian boundary, but may be applied to any rocks found to have such a widespread occurrence of similar conditions.

The Eagle Ford was determined to have been deposited under mostly anoxic conditions with short periods of oxic conditions throughout. The Eagle Ford in South Texas was found to have been subjected to more periods of euxinia during its deposition, but this statement should be taken with caution, as only one sample was used from South Texas. Statistically, one sample is meaningless, but it does lend encouragement and reason to do further studies from South Texas Eagle Ford.

5.2 Future Work

Since the use of and analysis of XRF data is still relatively new, there is much more work to be done to further the understanding of source rocks and their depositional environments. The construction of a database of XRF data should take place to facilitate the spread of data while encouraging more people to undertake the analysis. To expand on the data presented in this study, more samples need to be taken and analyzed from South Texas Eagle Ford. The Eagle Ford is proving to be a respectable reservoir in East Texas. More companies are beginning to drill wells in the Eagle Ford in East Texas, making it a prime area to be targeted for XRF analysis, potentially leading to better understanding of the rock, resulting in better wells.

This study was undertaken using only XRF data, supplemented to a minor degree by physical rock description. Although XRF is a useful tool for performing analysis of the rocks in question, it is not the only tool capable of enhancing the understanding of the rocks. It is recommended that total organic carbon (TOC) and total inorganic carbon (TIC) analysis should be performed to enhance the XRF data, while being useful in more detailed work concerning redox conditions and hydrocarbon generation capacities. Vitrinite reflectance studies are commonplace in the petroleum industry for determining the thermal maturity of any kerogens found in the rock, and would also serve to supplement the rock analysis. XRD analysis was not

performed on the cores, but could add data on the specific mineralogy of the rocks, even providing information about clay speciation. Clay speciation is important to know when drilling through a rock or trying to fracture-treat a reservoir. XRF falls short in this endeavor, as it can only identify approximate total clay volumes.

TOC analysis has proven useful in previous studies as a means of further analysis of many trace metals. Several trace elements have been shown to be associated with organic matter, specifically V (Breit and Wanty, 1991; Emerson and Huested, 1991; Morford and Emerson, 1999; Hetzel et al., 2009) and Mo (Algeo and Maynard, 2004; Algeo and Lyons, 2006; Algeo and Rowe, 2011; Rowe, Loucks, Ruppel, Rimmer, 2012).

REFERENCES

Algeo, T.J. and Lyons, T.W., 2006. Mo-total organic carbon covariation in modern anoxic marine environments: implications for analysis of paleoredox and paleohydrographic conditions. Paleoceanography, v. 21, p. 1016.

Algeo, T.J. and Maynard, J.B., 2004. Trace-metal behavior and redox facies in core shales of Upper Pennsylvanian Kansas-type cyclothems. Chemical Geology. 206: 289-318.

Algeo, T.J. and Rowe, H.D. 2011, In press. Paleoceanographic applications of trace-metal concentration data. Chemical Geology.

Assareh, E., Behrang, R., Assareh, R., Hedayat, N., 2011. Global Electricity Consumption Estimation Using Particle Swarm Optimization (PSO). World Academy of Science, Engineering and Technology. 79.

Barron, E.J., 1983. A warm, equable Cretaceous: the nature of the problem. Earth Science Rev. 19, 305-338.

Blakey, R., 2009. Paleogeography. http://jan.ucc.nau.edu/~rcb7/index.html

Breit, G.N., Wanty, R.B., 1991. Vanadium accumulation in carbonaceous rocks. A review of geochemical controls during deposition and diagenesis. Chemical Geology 91(1-2), 83-97.

Brumsack, H.J. 2006. The trace metal content of recent organic carbon-rich sediments: Implications for Cretaceous black shale formation. Palaeogeography, Palaeoclimatology, Palaeoecology. 232: 344-361.

Brumsack, H.J., 1989. Geochemistry of recent TOC-rich sediments from the Gulf of California and the Black Sea: Geologische Rundschau, v. 78, p. 851-882.

Calvert, S.E. and Pedersen, T.F. 1993. Geochemistry of recent oxic and anoxic marine sediments: implications for the geological record. Marine Geology. 113: 67–88.

Collier, R.W., 1985. Molybdenum in the northeast Pacific Ocean. Limnol. Oceanogr. 30, 1351–1354.

Colodner, D., Sachs, J., Ravizza, G., Turekian, K., Edmont, J., Boyle, E., 1993. The geochemical cycle of rhenium: a reconnaissance. Earth Planet. Sci. Lett. 117, 205–221.

Dehairs, F.,Chesselet,R., Jedwab,K., 1980. Discrete suspended particles of barite and the barium cycle in the open ocean. Earth Planet. Sci. Lett. 49, 528–550.

Dymond, J., Suess, E., Lyle, M., 1992. Barium in deep-sea sediment: a proxy for paleoproductivity. Paleoceanography 7, 163–181.

Emerson, S.R., Huested, S.S., 1991. Ocean anoxia and the concentrations of molybdenum and vanadium in seawater. Marine Chemistry 34(3-4), 177-196.

Fairbanks, M., 2012. High Resolution Stratigraphy and Facies Architecture of the Upper Cretaceous (Cenomanian-Turonian) Eagle Ford Formation, Central Texas. Master's Thesis. University of Texas at Austin. 1-119.

Goldberg, E.D., Arrhenius, G.O.S., 1958. Chemistry of Pacific pelagic sediments. Geochim. Cosmochim. Acta 13, 153–212.

Hetzel, A., Böttcher, M.E., Wortmann, U.G., and Brumsack, H.-J., 2009. Paleo-redox conditions during OAE 2 reflected in Demerara Rise sediment geochemistry (ODP Leg 207). Palaeogeography, Palaeoceanography, Palaeoecology 273(3-4), 302-328.

Hughes, E., 2011. Chemostratigraphy and paleoenvironment of the Smithwick Formation, Fort Worth Basin, San Saba County, Texas. Department of Geological Sciences Master's Thesis. University of Texas at Arlington. 1-93.

Jacobs, L., Emerson, S., Skei, J., 1985. Partitioning and transport of metals across the O2/H2S interface in a permanently anoxic basin: Framvaren Fjord, Norway. Geochim. Cosmochim. Acta 49, 1433–1444.

Jenkyns, H., 2010. Geochemistry of oceanic anoxic events. Geochemistry, Geophysics, Geosystems v 11 (March 2010).

Jones, B. and Manning, A.C. 1994. Comparison of geochemical indices used for the interpretation of palaeoredox conditions in ancient mudstones: Chemical Geology, v. 111, p. 111-129.

Koide, M., Hodge, V.F., Tang, J.S., Stallard, M., Goldberg, E.G., Calhoun, J., Bertine, K.K., 1986. Some comparative marine chemistries of rhenium, gold, silver and molybdenum. Appl. Geochem. 13, 705–714.

Kremling, K., 1983. The behavior of Zn, Cd, Cu, Ni, Co, Fe and Mn in anoxic Baltic waters. Mar. Chem. 13, 87–108.

Lea, D.W., Boyle, E.A., 1990. Foraminiferal reconstruction of barium distributions in water masses of the glacial oceans. Paleoceanography 5, 719–742.

Mancini, E.A. and Puckett, M., 2005. Jurassic and Cretaceous Transgressive Regressive (T-R) Cycles, Northern Gulf of Mexico, USA. Stratigraphy, Vol. 2, No. 1, 31-48.

Moore, T., and Scotese, C. R., 2012. *Ancient Earth: The Breakup of Pangea*, iPad application (app), Apple Computer, Cupertino, CA.

Morford, J.L., Emerson, S.E., 1999. The geochemistry of redox sensitive trace metals in sediments. Geochimica et Cosmochimica Acta 63(11-12), 1735-1750.

Rowe, H., Hughes, N., Robinson, K., 2012, The quantification and application of handheld energy-dispersive x-ray fluorescence (ED-XRF) in mudrock chemostratigraphy and geochemistry. Chemical Geology.

Schlanger, S.O., Jenkyns, H.C., 1976. Cretaceous oceanic anoxic events: causes and consequences. Geologie en Mijnbouw 55, 179-184.

Schlanger, S.O., Jenkyns, H.C., 1976. Cretaceous oceanic anoxic events: causes and consequences. Geol. Mijnb. 55, 179– 184.

Schmitz, B., 1987. Barium, equatorial high productivity, and the northward wandering of the Indian continent. Paleoceanography 2, 63–78.

Shaw, T.J., Geiskes, J.M. and Jahnke, R.A., 1990. Early diagenesis in differing depositional environments: the response of transition metals in pore water. Geochim. Cosmochim. Acta, 54: 1233-1246.

Simoneit, B.R.T., 1978. The organic chemistry of marine sediments. In: Riley, J.P., Chester, R. (Eds.), Chemical Oceanography. Academic Press, pp. 233–312.

Smith, C.N., and A. Malicse, 2010, Rapid handheld X-ray Fluorescence (HHXRF) analysis of gas shales: AAPG International Convention and Exhibition, Calgary, Alberta, Canada, 12-15 September 2010. (Extended Abstract) AAPG Search and Discovery Article #90108, 6 p.

Soua, M., 2011. Productivity and bottom water redox conditions at the Cenomanian-Turonian Oceanic Anoxic Event in the southern Tethyan margin, Tunisia. Revue méditerranéenne de l'environnement 4 (2011) pp. 653-664.

Tourtelot, H.A., 1979. Black shale: its deposition and diagenesis: Clays and Clay Minerals, v. 27, p. 313-321.

Tribovillard, N., Algeo, T.J., Baudin, F., Riboulleau, A., 2011. Analysis of marine environmental conditions based on molybdenum-uranium covariation – Applications to Mesozoic paleoceanography. Chemical Geology.

Tribovillard, N., Algeo, T.J., Lyons, T., and Riboulleau, A., 2006. Trace metals as paleoredox and paleoproductivity proxies: An update: Chemical Geology, v. 232, p. 12-32.

Turgeon, S., Brumsack, H.J., 2006. Anoxic vs Dysoxic events reflected in sediment geochemistry during the Cenomanian-Turonian Boundary Event (Cretcaeous) in the Umbria-Marche Basin of central Italy. Chemical Geology 234 (2006). pp 321-339.

Wedepohl, K.H., 1971. Environmental influences on the chemical composition of shales and clays. In: Ahrens, L.H., Press, F., Runcorn, S.K., Urey, H.C. (Eds.), Physics and Chemistry of the Earth vol. 8, Pergamon, Oxford (1971), pp. 305–333.

BIOGRAPHICAL INFORMATION

Brett Huffman was born on January 20, 1978 in Omaha, Ne. He moved to different states during his childhood, being the son of an Air Force officer. Brett graduated from Crowley High School in 1996 and went directly into college from there. He took a freshman level geology class and knew that was what he wanted to do. He graduated from Tarleton State University with a BS Geology and a minor in Biology. After graduation, he took a job with a small oil and gas exploration company and began to learn the petroleum industry. After working for the same company for three years, he took a ten month hiatus from oil and gas to work for an environmental company. He realized that while environmental was interesting, his true passion was working in the petroleum industry. He went back to work in oil and gas again for his previous company, working there until the demise of the company in early 2011. Realizing the company was in trouble, he chose to go back to graduate school at UTA in August 2010, seeking a MS Geology in order to be more marketable and be able to compete with other geologists who had obtained a MS degree. He began working under the supervision of Dr. Rowe in early 2012, beginning work on his thesis. Brett was hired by an oil and gas company in Fort Worth named Energy & Exploration Partners as a full time intern. He expects to graduate in August, 2013 and move from intern to full geologist status. He remains optimistic and excited about his career in oil and gas, hoping that his research will become more commonplace, as he has learned some of the many benefits of utilizing XRF data in petroleum exploration.